March 14, 2018

REPORT #E18-304

Secondary Glazing System (SGS) Moisture Analysis and Validation

Prepared For NEEA:
Rob Curry, Sr. Project Manager

Prepared by:
Robert Hart

Ernest Orlando Lawrence Berkeley National Laboratory
1 Cyclotron Rd.
Berkeley, CA 94720
510-486-4000

Northwest Energy Efficiency Alliance
PHONE
503-688-5400
EMAIL
info@neea.org

Disclaimer

1. EXECUTIVE SUMMARY

A refined methodology for simulating the hygrothermal conditions adjacent to and on glass surfaces is developed and performed for nine products as an extension to the work presented in *Secondary Glazing System (SGS) Thermal, Solar, and Energy Performance Analysis and Validation* (Hart 2005). Extensions to Berkeley Lab THERM and WINDOW software tools are implemented and we introduce the concept of condensation resistance of unsealed gaps (CRU) indices as a companion to the existing NFRC CR ratings. These models are validated through experiments by local temperature and moisture propagation measurements, and therefore provide accurate determination of CRU at predetermined humidity ratios.

The reported CRU numbers seem to be mostly on the very low end (i.e., very poor performance) for all unsealed units due to the use of humidity ratios that are representative of indoor room air. This indicates that further research might be needed to establish expected moisture content in unsealed gaps for different product types and to relate them to indoor room air, so that more representative CRU procedure can be developed.

Four SGS systems are measured for air leakage and moisture propagation performance. The results vary greatly between products; from preventing all air leakage and most moisture transfer to no resistance to air or moisture transfer. The measured performance data is combined with the results of Energy Plus annual energy simulations to determine trends and relative condensation performance of nine SGS products. We make the assumption that there are no moisture sources or sinks, and there is no liquid transport flux. Both of these assumptions are significant in that condensed moisture is considered out of the system, potentially misjudging the condensation time. With these assumptions and knowing that all buildings are controlled and perform differently, the results presented here should be viewed only as indicators of relative performance between SGS products and not absolute condensation potential.

The results show that all SGS systems containing unsealed glazing cavities increase condensation risk over single pane base windows. Condensation risk is highest on north facing surfaces, and lowest on east facing, but the time difference is relatively small. Condensation also occurs most often during unoccupied hours. Finally, low water vapor diffusion resistance factors to the outside coupled with high room-side resistance typically results in the fewest condensation hours, while the opposite case (high resistance to the outside and low resistance room-side) results in the greatest number of condensation hours.

Future work should include installation and monitoring of SGS in real buildings to validate the simulation results. The CRU metric is introduced as a preliminary step with the long-term goal of a standardized metric for condensation potential of SGS and other attachment products. Further development of the CRU metric should be done to ensure all significant aspects of SGS design, such as resistance to air leakage

and moisture transfer, are considered and presented fairly with respect to the existing CR standards.

2. INTRODUCTION

Background

The Northwest Energy Efficiency Alliance (NEEA) is interested in accelerating the adoption of energy-saving building envelope products. The market NEEA is most interested in relative to secondary glazing systems (SGS) consists of existing multi-story office buildings with single glazed, non-thermally broken aluminum window frames constructed between the mid-1950s and the mid-1980s. For this project, SGS products are defined as one or more pane glazing units designed for insertion into existing commercial storefront or curtain wall systems with monolithic glazing. The SGS is installed from the interior with the intent of improving the thermal performance of the existing glazing system.

Condensation has been a persistent and often misunderstood problem associated with windows. It occurs when the surface temperature of a window component drops below either the dew point or frost point of the air adjacent to the surface. In cold climates, single-glazed windows characteristically suffer from water condensation and the formation of frost on the inside surface of the glass in winter.

Condensation can also be a problem on the interior surfaces of window frames. Metal frames, in particular, conduct heat very quickly, and will "sweat" or frost up in cool weather. Solving this condensation problem was a major motivation for the development of thermal breaks for aluminum windows. Infiltration effects can also combine with condensation to create problems. If a path exists for warm, moisture-laden air to move through or around the window frames, the moisture will condense wherever it hits its dew point temperature, often inside the building wall. Frames must be properly sealed within the wall opening to prevent this potential problem. In some instances, the infiltration air will be dry, such as on cold winter days, and it will thus help eliminate condensation on the window surfaces.

Condensation risk has been identified by NEEA as a potential barrier to broad SGS market penetration. Some building analysis software, such as WUFI (Fraunhofer 2001), attempt to predict moisture transfer and condensation in buildings. These tools though are not directly applicable to SGS products. The condensation potential of SGS systems in real buildings is unknown.

A report titled *Secondary Glazing System (SGS) Thermal, Solar, and Energy Performance Analysis and validation,* by R. Hart et. al. was produced in 2015 as a first step in the analysis of SGS. The report established an initial database of SGS product performance. This report expands that research into moisture transfer and condensation resistance of SGS. There are multiple objectives to this report, the most substantial being a refined methodology for simulating the hygrothermal conditions adjacent to and on glass surfaces. Extensions to Berkeley Lab THERM and

WINDOW software tools are implemented and we introduce the concept of condensation resistance of unsealed gaps (CRU) indices as a companion to the existing NFRC CR ratings. These models are validated through experiments by local temperature and moisture propagation measurements. A methodology for predicting condensation through annual energy modeling software is developed and used to predict condensation in DOE prototype commercial buildings for nine SGS products.

Product definitions

The nine products analyzed in this report are the same products defined in the previously mentioned LBNL report and its appendices (Hart 2015). A single clear glazed non-thermally broken aluminum commercial storefront window frame is used as the baseline glazing system. It is designated as representative of commercial windows constructed between the mid-1950s and the mid-1980s. The group of SGS products simulated represents the diversity of current commercially available products.

All tested SGS use glass as the primary glazing material. Glazings vary from single pane glass to triple pane with a suspended center layer film. A minimum of one low-e coating is present in all systems; with the most insulating products utilizing insulated glazing units (IGU) and multiple low-e coatings. Most systems support the glazing with aluminum framing that attaches directly to the inside dimensions of the base window, while one product attaches directly to the base window glass and another mounts external to the base frame. Alphabetic designations are used throughout this report in order to maintain anonymity of tested SGS.

All tested SGS products create an insulating air space between the base window glass and the SGS glass. For the purposes of condensation resistance, only hermetically sealed and desiccated cavities are considered sealed. All cavities that are not hermetically sealed nor desiccated are considered unsealed, meaning they allow moisture to transfer from either the room-side or exterior environment.

Governing equations

Moisture transfer through windows primarily occurs by moist air movement and diffusion. Moist air movement occurs through leaks and cracks in the frame-wall, frame-glazing, and frame-sash interfaces. The driving mechanism for moist air movement through windows is the air pressure difference from interior to exterior surfaces. Pressure across the building envelope occurs from air density gradients driven by indoor-outdoor temperature differences, bouncy (stack effect) in tall buildings, wind, and unbalanced mechanical systems. Flow through building components can typically be described by the power law equation (Eq. 1). Equations 2 and 3 relate air volume in the power law equation to moisture [ASHRAE 2009].

$$\dot{V} = c(\Delta P)^n \qquad [1]$$

$$V = \frac{m_a + m_w}{\rho} \quad [2]$$

$$W = \frac{m_w}{m_a} \quad [3]$$

where

V	[m^3]	air volume
$\dot{V}$	[m^3/s]	air flow rate
c	[$m_3/s\text{-}Pa^n$]	flow coefficient
n	[-]	pressure exponent
P	[Pa]	ambient air pressure
ρ	[kg/m3]	air density
m_w	[kg]	mass water vapor
m_a	[kg]	mass air
W	[kg_w/kg_a]	Humidity ratio

Moisture diffusion is driven by the gradient of water vapor partial pressure in the air. Diffusion of moisture from areas of high concentration to low concentration only becomes significant when little to no air movement occurs. Fick's Law, or the moisture diffusion equation, is used to predict moisture vapor diffusion. This equation (eq. 4) is analogous to the heat equation or Fourier's Law. Equations 5 and 6 relate vapor diffusion to water vapor partial pressure, air pressure, and temperature [Kunzel 1995].

$$\frac{\partial w}{\partial t} = -\nabla \cdot (g_w + g_v) + S_w \quad [4]$$

where

$$g_v = -\frac{\delta}{\mu} \nabla P_w \quad [5]$$

$$\delta = 2.0 \cdot 10^{-7}\, T^{0.81}/P \quad [6]$$

t	[s]	time
g_w	[kg/m^2s]	liquid transport flux density
g_v	[kg/m^2s]	vapor diffusion flux density
S_w	[kg/m^2s]	moisture source or sink
δ	[kg/msPa]	water vapor diffusion coefficient in air
μ	[-]	water vapor diffusion resistance factor
P_w	[Pa]	water vapor partial pressure
T	[K]	ambient air temperature

Condensation forms at the coldest locations, typically the lower corners or edges of an insulated product even when the center of glazing is above the limit for condensation. Generally, as the insulating value of the glazing is improved, the area where condensation can occur is diminished. With SGS products though, condensation potential may increase with the insulating value of the product. This is because the temperature of the glass closest to the exterior becomes colder and is

adjacent to an un-desiccated air space. Condensation potential increases as the outdoor temperature is lowered and the indoor relative humidity increases.

NFRC has developed a condensation resistance (CR) value for rating how well a fenestration product can resist the formation of condensation on the room side surface of the product at a specific set of environmental conditions. The CR calculation method is defined in the NFRC 500: Procedure for Determining Fenestration Product Condensation Resistance Values (National Fenestration Rating Council, 2013). The condensation resistance model outlined in NFRC 500 is developed around condensation on room-side exposed surfaces because factory-sealed insulated glazing utilizes a permanent seal to prevent the introduction of moisture between glass. The void may be filled with air or dry gases, such as argon. A desiccant material in the edge spacer between the panes is used to absorb any residual moisture in the unit when it is fabricated or any small amount that might migrate into the unit over many years. NFRC 500 and its accompanying user guide NFRC 501 (National Fenestration Rating Council, 2013) contain more information about condensation resistance.

The NFRC CR rating is designed for comparison of room side condensation potential. The condensation resistance of unsealed gaps (CRU) procedure developed in this report is intended to do the same for products with unsealed glazing cavities, such as SGS. The important assumption made in the development of CRU is that same humidity content of air was assumed as in CR determination (30%, 50%, and 70% RH at 70 F), so that numbers are better comparable to CR.

3. ANALYSIS PROCEDURE

Air movement, local temperatures, and moisture diffusion into and through SGS must be characterized in order to describe moisture propagation and condensation resistance. The measurement and simulation analysis procedures described in the following section detail the methods used in this report.

Measurements

Air movement, local temperatures, and moisture diffusion are measured independently using three different measurements procedures described in the following sections.

Air movement

AAMA/WDMA/CSA 101/I.S.2/A440 [AAMA 2008] defines air leakage resistance criteria new fenestration products must meet for qualification in the US. This standard though is not necessarily representative of the SGS target market of installed single-pane aluminum windows. To determine typical air leakage, we measure a baseline system as well as several assembled SGS utilizing the standard test method for measuring air leakage for windows defined in ASTM E283 [ASTM 2012]. Airflow measurements are taken for a range of pressures between 50 Pa and

230 Pa. The pressure used for rating residential (R) windows at 75 Pa is included. The higher 300Pa pressure for rating architectural (AW) windows was not achievable in all cases with our test equipment and is therefore omitted. Measurements are performed with the Wind Maker PLUS test kit manufactured by the RM Group. Figure 1 illustrates the laboratory set-up. Calibration is performed with the Wind Maker Calibration Box manufactured to the AAMA 204-98 [AAMA 1998] specifications. The results from this test are presented in the form of volumetric flow rate per unit window area, q [L/s-m^2], as a function of differential pressure, P [Pa].

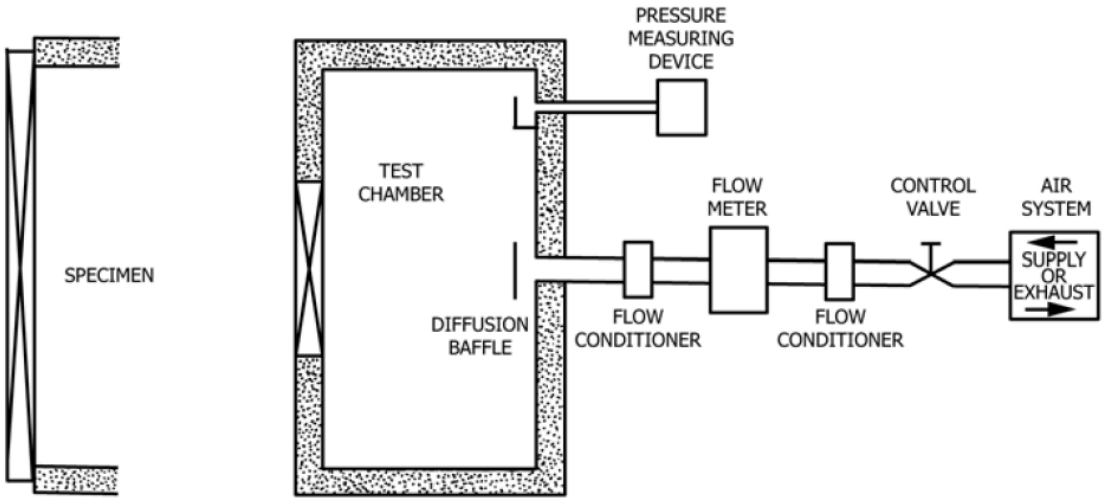

Figure 1. Schematic of laboratory window air leakage measurements [ASTM 2012]

Local Temperatures

The simulated CR and CRU values are highly dependent on accurate prediction of surface temperatures. To verify simulated surface temperatures, the base window and a selection of four SGS systems were tested in the LBNL laboratory over a range of outdoor temperatures from 15C to -15C with the room temperature held at a constant 21C. Thermocouples were placed at the COG and EOG of surface #2, on the frame in the unsealed cavity space, and the COG and EOG of the room side surface. A typical example of the thermocouple placement is given in Figure 2.

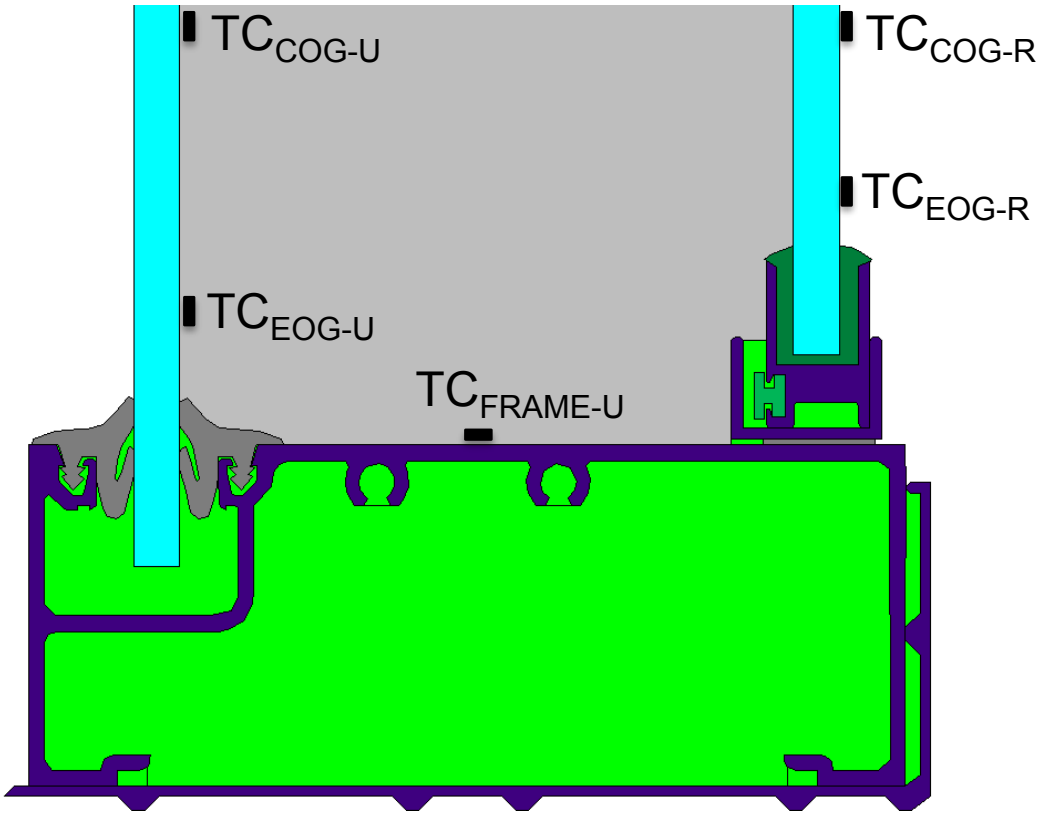

Figure 2. Typical thermocouple (TC) placement for validation testing

Moisture transfer

There is no window industry standard for measuring moisture diffusion and existing standard procedure structures, such as ISO 12572 [ISO 2001], are impractical for window systems. A new procedure is therefore used in this report. As previously discussed, Fick's law governs moisture diffusion, where the moisture flux is proportional to the concentration difference. This law is analogous to Fourier's Law for heat conduction, where the heat flux is proportional to the temperature difference. For heat transfer the proportionality constant is defined as the thermal conductivity, while in moisture transfer it is defined as the permeability. Our goal is to determine the water vapor permeability of the SGS systems as a function of the average water vapor partial pressure, P_w, between the indoor and outdoor environment. For the purposes of our analysis, we will represent the permeability as μ, or the water vapor diffusion resistance factor as defined in Equation 5. μ is a convenient term for analysis and describes the ratio of diffusion through a material to the diffusion of moisture in air at a given temperature and pressure.

The measurement method we use is analogous to typical procedures for thermal testing. To begin testing, the system is allowed to come into equilibrium. The moisture content in one space is then adjusted suddenly by the introduction or removal of water vapor to disrupt the balance. Humidity and temperature sensors

are installed on both sides of the window and within the unsealed glazing cavity to monitor the state of each air space. We record these values in order to calculate the partial pressures on all sides of the SGS as functions of time. The rate of change of moisture in the gap is correlated to the partial pressure difference to determine the permeability.

An important aspect of diffusion testing is to minimize air mass transfer. As previously stated, the transfer of moist air mass typically dominates moisture transfer when it occurs. Controlling the pressure differential across the unit removes the driver for air mass transfer. This is accomplished by maintaining thermal and air pressure equilibrium on both sides of the window.

The water vapor diffusion resistance factor, μ, is determined from the test results utilizing the procedure described schematically in Figure 3, where ϕ is the relative humidity. Calculations for space properties are per ASHRAE 2009, and μ is solved for with equation 7 where diffusion occurs between only two spaces:

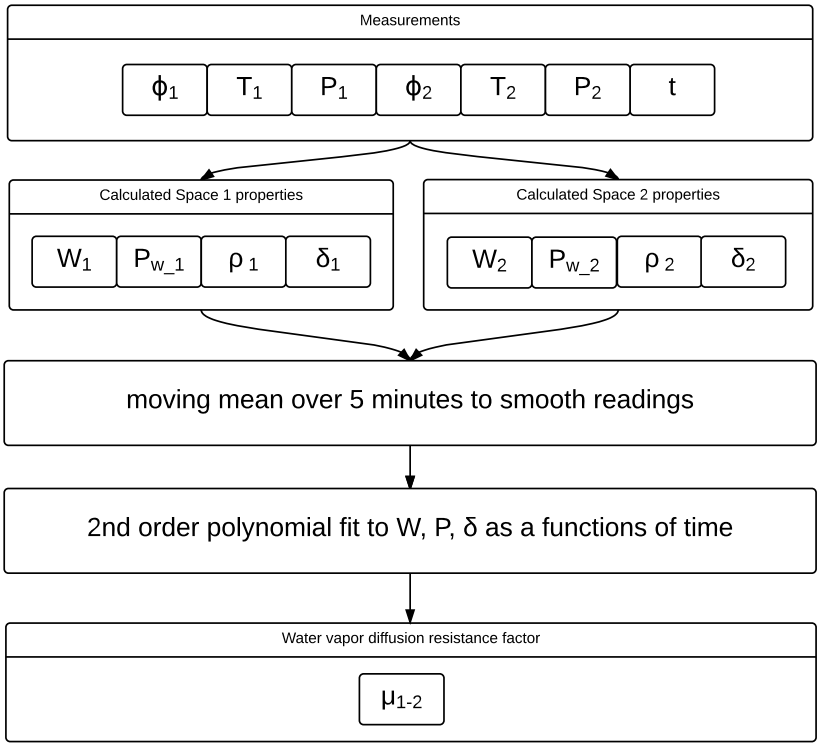

Figure 3. Schematic of water vapor diffusion resistance factor calculation from measurements

Simulation

Simulation is performed to determine when condensation with SGS might occur as a standardized product comparison via the CRU metric and in real buildings with annual energy simulations.

Condensation Resistance for Unsealed Glazing Gaps (CRU)

The NFRC CR value is an indicator of condensation performance on the interior, or room side, surface of a product only. A new model, called the condensation resistance for unsealed glazing gaps (CRU), is developed as part of this report. The primary differentiators between the models are shown in Figure 4. The NFRC CR surfaces are adapted to include the left and right sides of each unsealed gap and the frame surface between them.

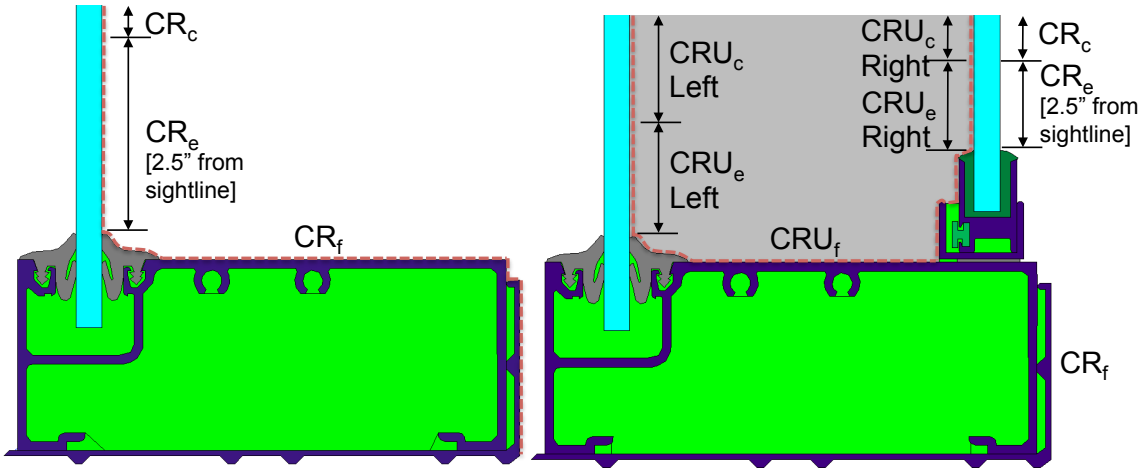

Figure 4. A) NFRC 500 CR areas. B) Proposed CRU areas

When implementing the CRU model there are two simulation limitations that must be considered. First, the model is based on the assumption that the unsealed air space can be represented as a sealed cavity with a convection air loop. Our validation testing confirms that the sealed model assumption is suitable for all products examined in this report. Second, the model assumes non-glazing surfaces within the unsealed gap are adiabatic (no heat transfer through the surface). Figure 5 illustrates this area. In practice, this assumption results in simulated frame temperatures higher than real windows because the cold wash of air resulting from the convection loop on the outer glass pane to the frame surface is not accounted for. The EOG surface is typically of greatest concern, but in certain configurations the frame surface may be the condensation driver and condensation potential will be under predicted. For the validation cases examined in this project, the predicted frame temperature was 1.5C warmer on average than measured temperature.

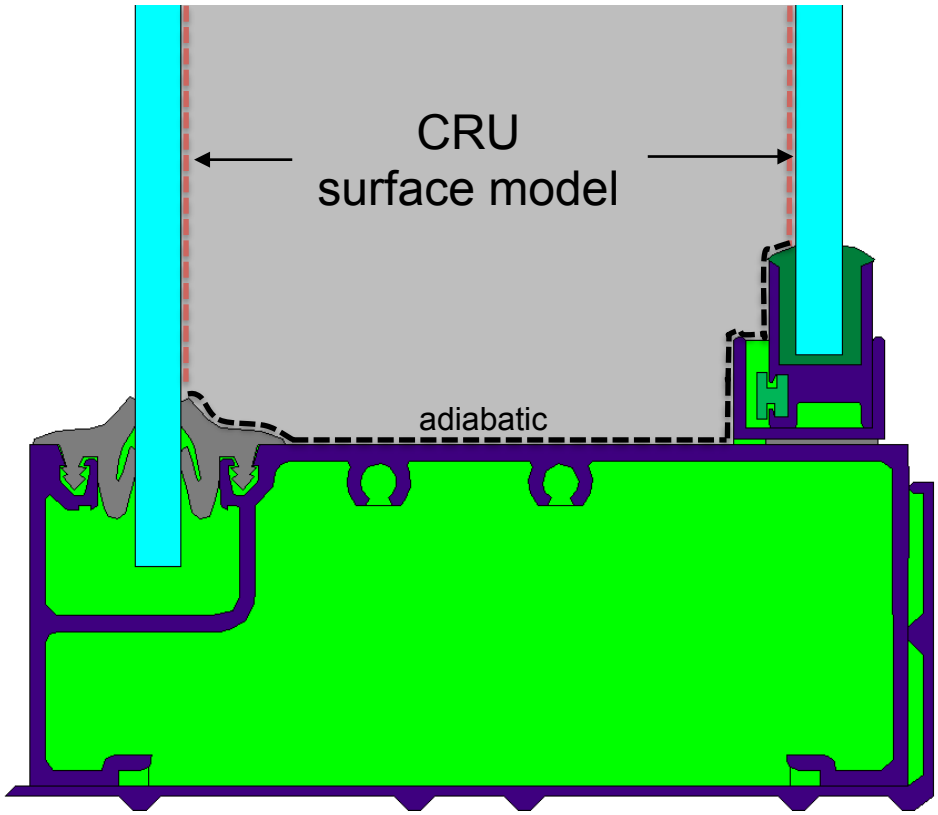

Figure 5. Surfaces marked with black dashed line are adiabatic in the CRU model.

Whole building

Our procedure is broken into two steps; first whole building energy analysis is performed in 15-minute time steps for one representative year, then the simulated environmental conditions at each time step are used to simulate the expected moisture content and if condensation risk in SGS for the same time steps of the representative year. All buildings are unique, therefore the results presented here are meant for comparative analysis between similar products and should not be considered as indicators of actual performance in any one particular building.

EnergyPlus is an energy analysis and thermal load simulation program. Based on the description of a building, EnergyPlus calculates heating and cooling loads necessary to maintain thermal control set points. Simultaneous integration of these—and many other—details verify that the EnergyPlus simulation performs as a real building would (U.S. Department of Energy, 2013).

The DOE, in conjunction with three of its national laboratories, has developed commercial reference buildings. These reference buildings provide complete descriptions for whole building energy analysis using EnergyPlus simulation software. There are 16 building types that represent approximately 70% of the commercial buildings in the U.S. These modules provide a consistent baseline of

comparison. Reference buildings are provided for new construction, existing buildings constructed after 1980, and existing buildings constructed before 1980 (US Department of Energy).

In addition to the 16 building types, 16 climate zones, which represent all U.S. climates, were used to create the reference buildings. The climates are simulated using typical meteorological year (TMY) data sets derived from the 1961-1990 and 1991-2005 National Solar Radiation Data Base archives. The TMY3s are data sets of hourly values of solar radiation and meteorological elements for a 1-year period. Because they represent typical rather than extreme conditions, they are not suited for designing systems to meet the worst-case conditions occurring at a location (The National Renewable Energy Laboratory, 2015).

The EnergyPlus prototype buildings and climates investigated in this study were selected to match NEEAs requirements based on their target market for the SGS products. Table 1 summarizes the selected building and climate simulation parameters.

Table 1. EnergyPlus prototype building parameters

Parameter	**Description**
Construction type	Existing buildings constructed before 1980 ("pre-1980")
Building type	Large Office Medium Office Small Office
Climate zone	Zone 3: Oakland, CA Zone 4: Portland, OR Zone 5: Spokane, WA Zone 6: Missoula, MT

The three building types and four climate zones combine with nine window options for a total of 108 annual energy simulations. All building HVAC systems are sized for the base window system then the simulations are rerun with each SGS product.

Surface condensation occurs when a surface temperature is at or below the dew point temperature of moist air adjacent to that surface. To predict condensation of an SGS product as a function of time in EnergyPlus, we therefore determine the surface temperature of each surface and the dew point temperature of the air adjacent to that surface at every time step we are interested in. If the dew point temperature of the adjacent air is below that of the surface we assume condensation occurred for the entirely of that time step. A granularity of 15-minutes is used in the EnergyPlus simulations.

Surface temperature is determined in EnergyPlus using the Complex Fenestration Calculation Module with window input BSDF idf files generated in Berkeley Lab WINDOW and THERM (Mitchell 2013). Use of this module allows for 15-minute time

step center-of-glass (COG) temperature output for each glazing surface in the SGS. An important assumption made in this analysis is that the COG is the lowest temperature on each surface. Analysis presented in this report shows that the edge-of-glass (EOG) in SGS products is typically colder than COG and by as much as 1.5 °C in extreme indoor-outdoor temperature gradients. The COG surface temperature assumption therefore reduces the total overall predicted condensation time for nearly all SGS products.

Exterior dew point temperature is an input from the TMY weather data. Interior zone dew points are calculated by EnergyPlus based on the input weather, HVAC, building properties, etc. Dew points in the unsealed glazing cavities common with SGS products is performed after the completion of the EnergyPlus simulation using the process described schematically in Figure 6. A detailed step-by-step description of the algorithm and the equations used is provided in Appendix 1.

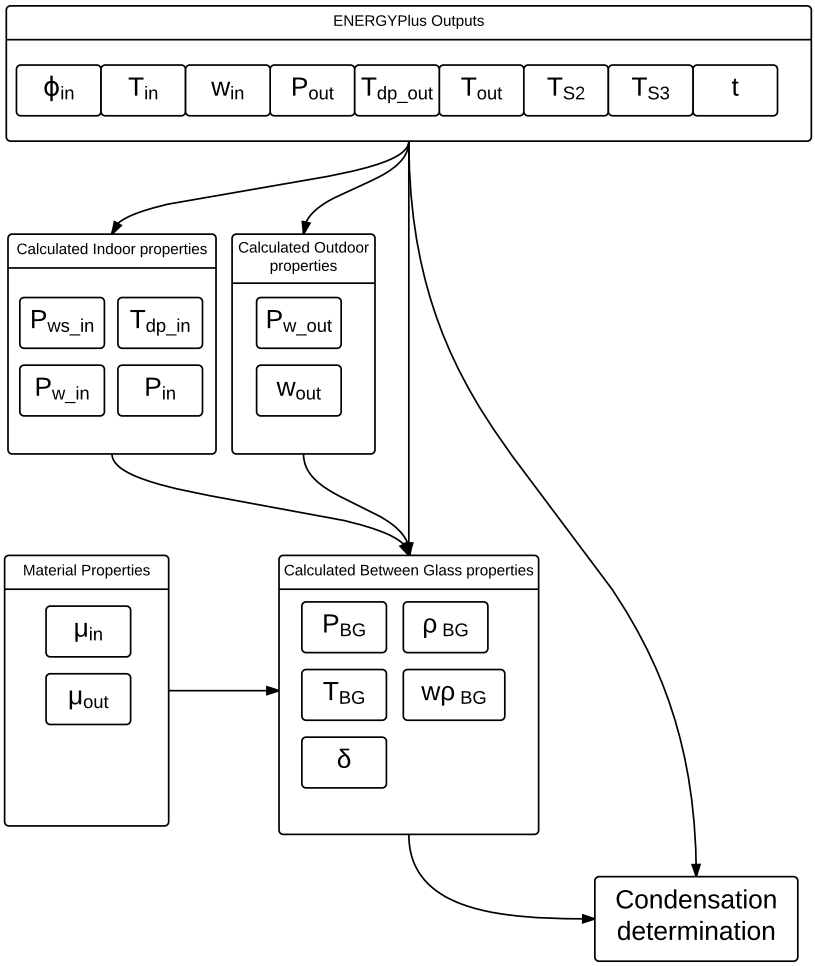

Figure 6. Schematic of algorithm to determine surface condensation from EnergyPlus outputs

The process is to compute the required indoor and outdoor moist air properties for each time step based on the EnergyPlus outputs. Then, starting from the first data point in the set, (January 1 at 00:15 in this work) calculate the expected between glass moist air properties of the next time step iteratively. Equations 7 – 9 are the fundamental equations used in the iterative process. Equation 7 is based on Equation 4 with the assumptions that there are no moisture sources or sinks, and there is no liquid transport flux. Both of these assumptions are potentially significant in that condensed moisture is considered out of the system, potentially underestimating the condensation time. Equation 8 is identical to Equation 6, and Equation 9 is used to determine the between glass partial water pressure used as an input in the next time step of the iteration.

$$(W \cdot \rho_a)_{t2} = (W \cdot \rho_a)_{t1} + \delta(t_2 - t_1)\left[\left(\frac{P_{w\_in} - P_{w\_BG}}{\mu_{in} \cdot \Delta x^2}\right)_{t1} + \left(\frac{P_{w\_out} - P_{w\_BG}}{\mu_{out} \cdot \Delta x^2}\right)_{t1}\right] \quad [7]$$

$$\delta = 2.0 \cdot 10^{-7} \, (T_{BG}^{0.81})_{t2} / (P_{BG})_{t2} \quad [8]$$

$$P_{W\_BG} = \frac{P \cdot W_{BG}}{(0.621945 + W_{BG})} \quad [9]$$

Figure 7 shows box plots of the outdoor-indoor air pressure differential for each 15-minute time step of the TMY grouped by each location and building type. The mean and quartiles of the pressure differential range from 0 to 5 Pa and would result in insignificant pressure driven airflow through SGS systems. Therefore, moist air movement through the SGS systems is assumed negligible and is not considered in the condensation analysis.

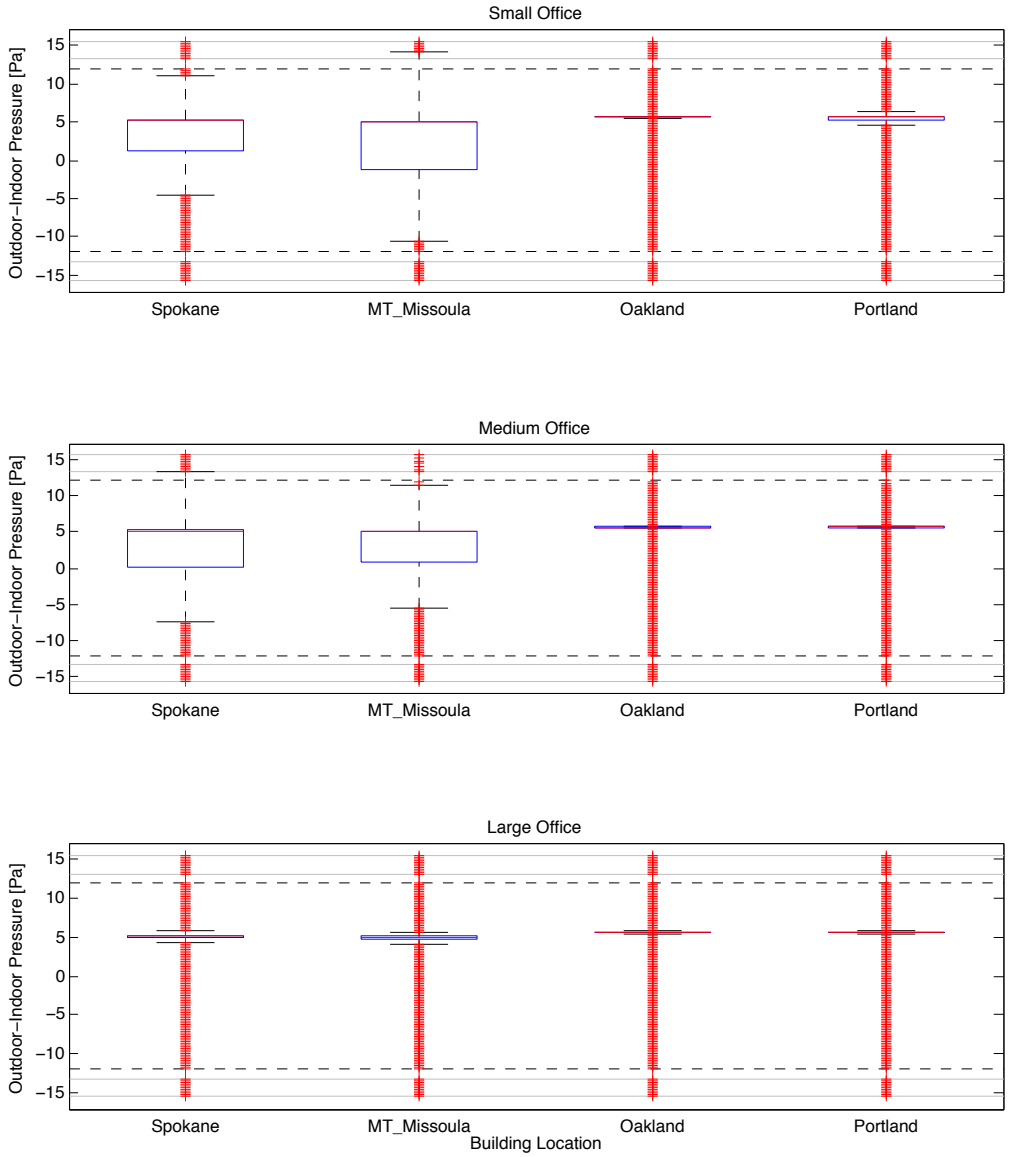

Figure 7. Box plots of outdoor-indoor pressure difference for each 15-minute timestep

Our technique of determining between-glass moist air properties after the EnergyPlus simulation is completed requires that indoor spaces are so large that the simulated moisture mass into and out of the between glass SGS space for all SGS in an interior zone has insignificant impact on the overall interior zone moisture content. Comparing the total moisture mass into and out of the SGS to the total moisture content in the zones checks this assumption. Figure 8 shows box plots of this ratio for all time steps considered in the study. On average, the change in SGS between-glass moisture mass is approximately 3e-6 percent of the total room moisture mass. The given assumption therefore has insignificant impact on the simulation accuracy.

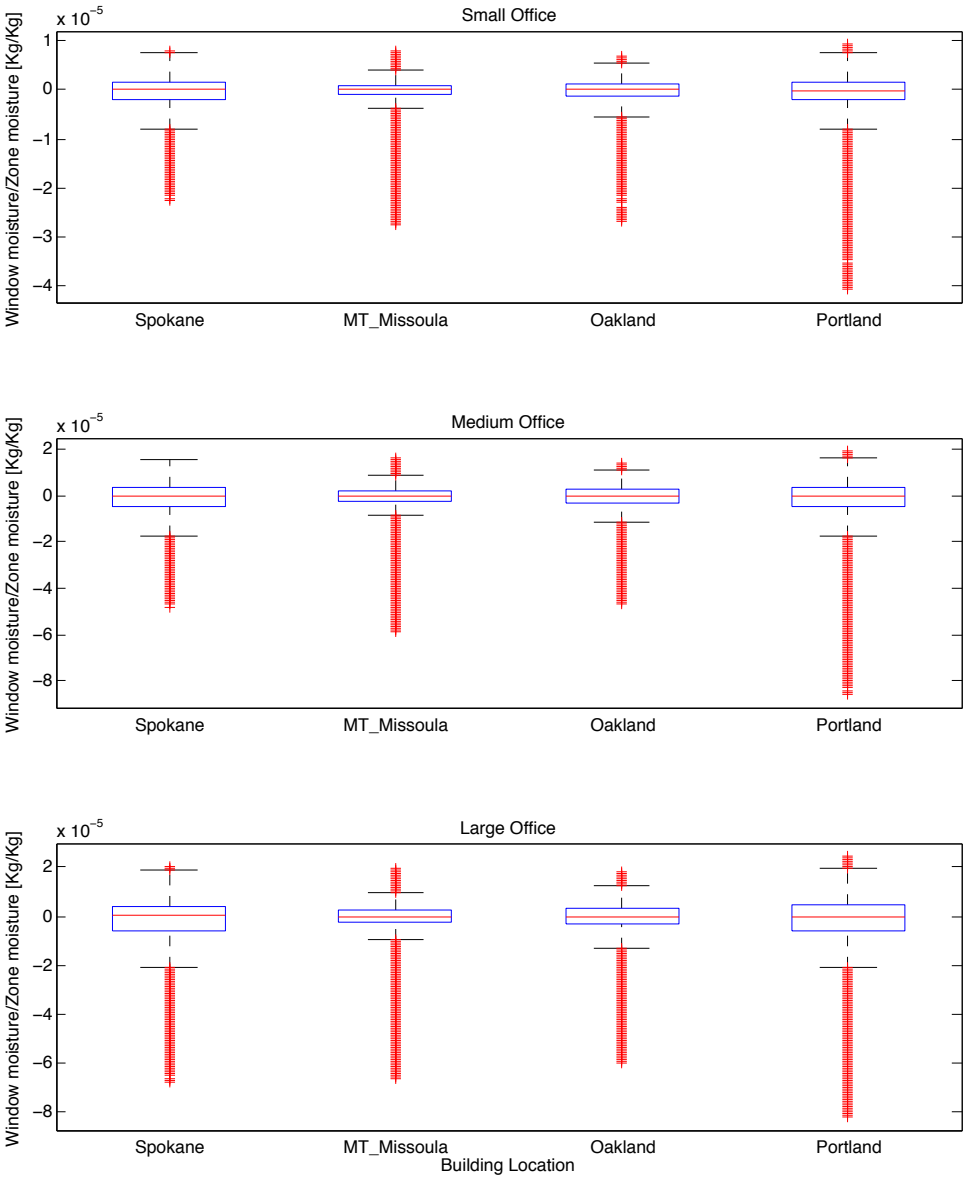

Figure 8. Ratio of moisture content in Zone to moisture change in SGS.

4. RESULTS

The following section outlines the results from our measurements and simulations.

Measurements

Air movement

Initial airflow measurements with base frame only resulted in negligible flow through the window. This result is expected and typical for new fixed type frames such as the baseline window used for this study. In order to quantify the impact of SGS on air leakage, leakage paths are artificially introduced into the base frame by

removing multiple sections of glazing seal at the head and sill on both sides of the glazing. The modified base frame construction remained untouched for the remainder of air leakage testing.

Window air leakage is typically reported as an absolute volume of flow per area of window. As add-on products though, SGS performance cannot be accurately measured without a defined baseline. Since no baseline window or air leakage is currently defined for SGS, our analysis presents results as a percent reduction in air leakage volume per area of window. This allows for easy comparison between products. Figure 9 shows the percent air leakage improvement for all tested products over a range of pressures. At the extremes of performance, Product G eliminated all air leakage for the entire range of pressures measured, while Product A had no measureable impact to leakage. Product E showed flow reduction ranging between 50 – 70 percent, and Product I was less effective with 0 – 30 percent reduction in air leakage. The flow resolution of our test equipment is the primary reason for the large jumps in performance seen in Product I.

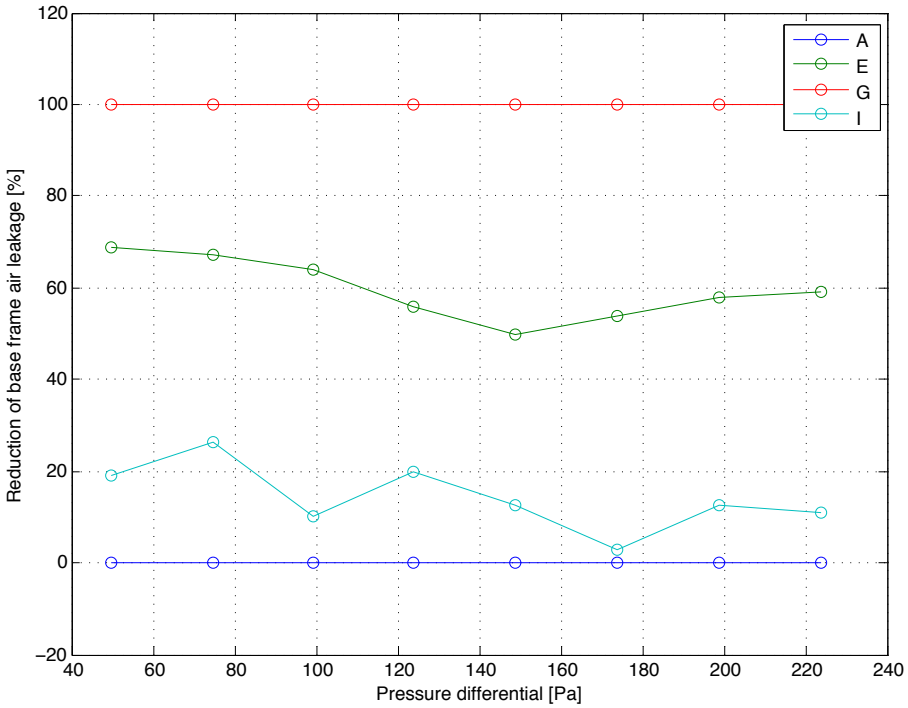

Figure 9. Reduction in air leakage of SGS products compared to base frame

Local temperatures

Cold side conditions were held for a minimum of one hour in 5C increments between 15C and -15C. Figures 10 - 14 show the simulation predicted surface temperatures compared to the measured surface temperatures for four cases: Base, H, G, A, and I respectively. The Base frame is single glazing and therefore only room side surface temperatures are recorded and a NFRC CR is possible to generate while

a CRU number is not. The results show agreement between simulated and measured performance within 1C throughout.

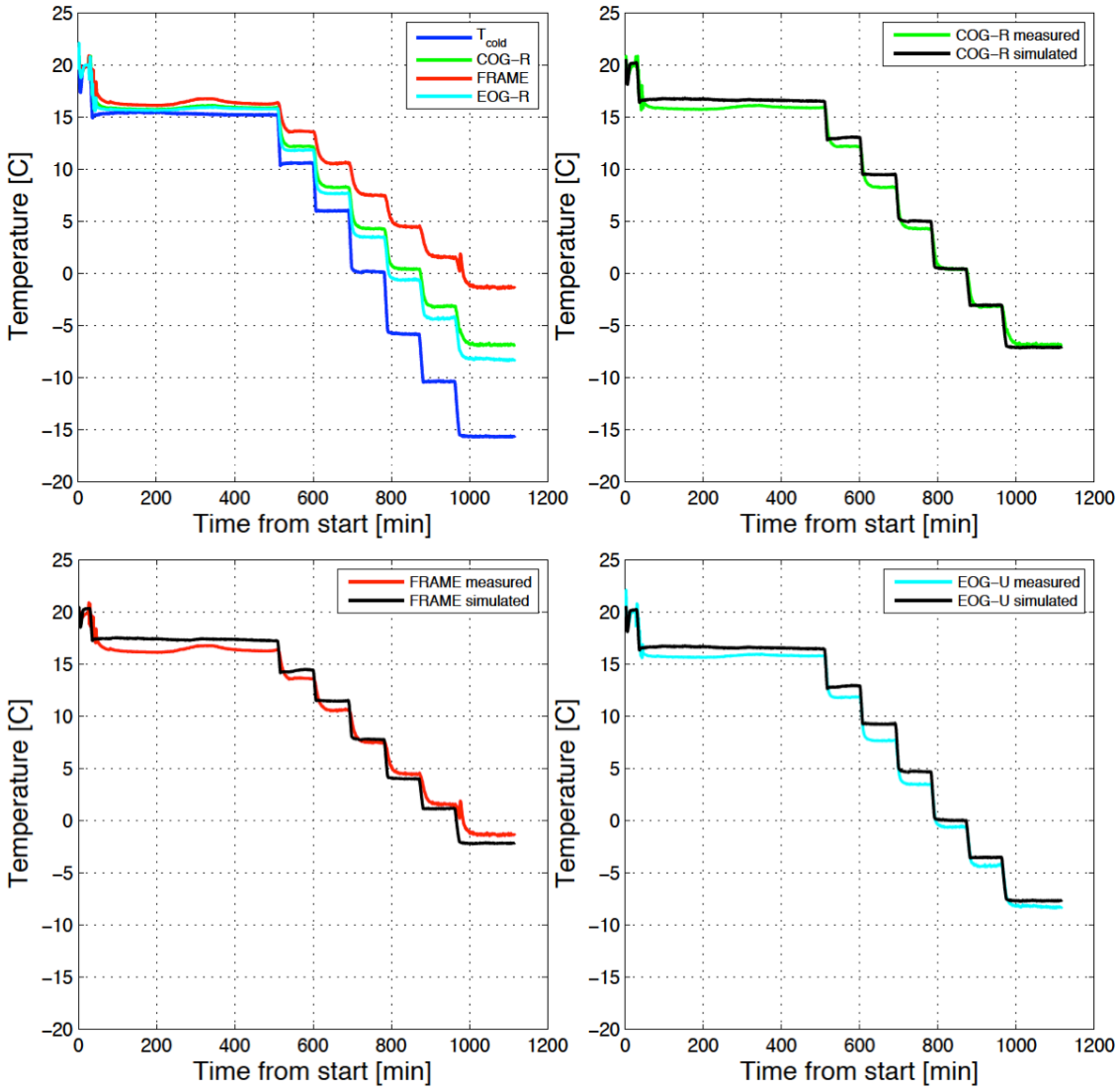

Figure 10. Measured surface temperatures on base window

Product H in Figure 11 creates a triple pane IGU by sealing and desiccating the air space between the base window and SGS glazing. Thus, the NFRC CR calculation methodology used for the base window applies to this product as well. The created triple pane IGU is highly insulating so the time to reach steady state temperatures on most surfaces is greater than the allotted three hours at each cold side condition. The extended duration at the final cold side state though shows that the simulated and measured surface temperatures again match within 1C for all surfaces.

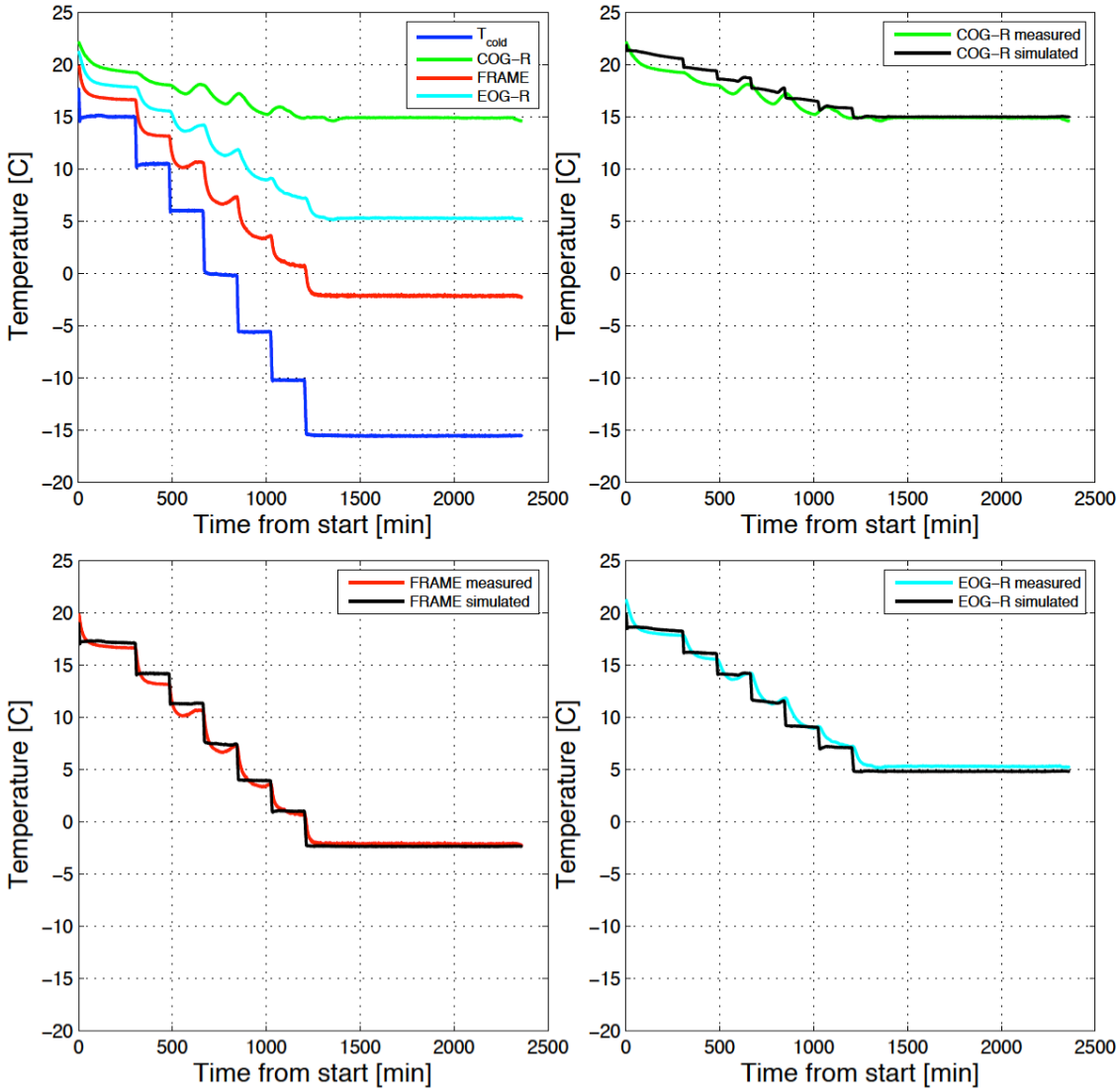

Figure 11. Measured surface temperatures on product H

Products G, A, and I in Figures 12 - 14 introduce the use of the newly developed CRU model. The COG-U and EOG-U temperatures match within 1C, similar to the NFRC CR models above. The FRAME temperatures though are not within this tolerance, and differences of up to 2C shown. This discrepancy is the result of using an equivalent conductivity for the gas space below the top most base frame sight line. The explanation for this simulation method is given in the previous section. The equivalent conductivity assumption always results in under prediction of the sill frame temperature (in cases where T_{cold} is less than T_{room}).

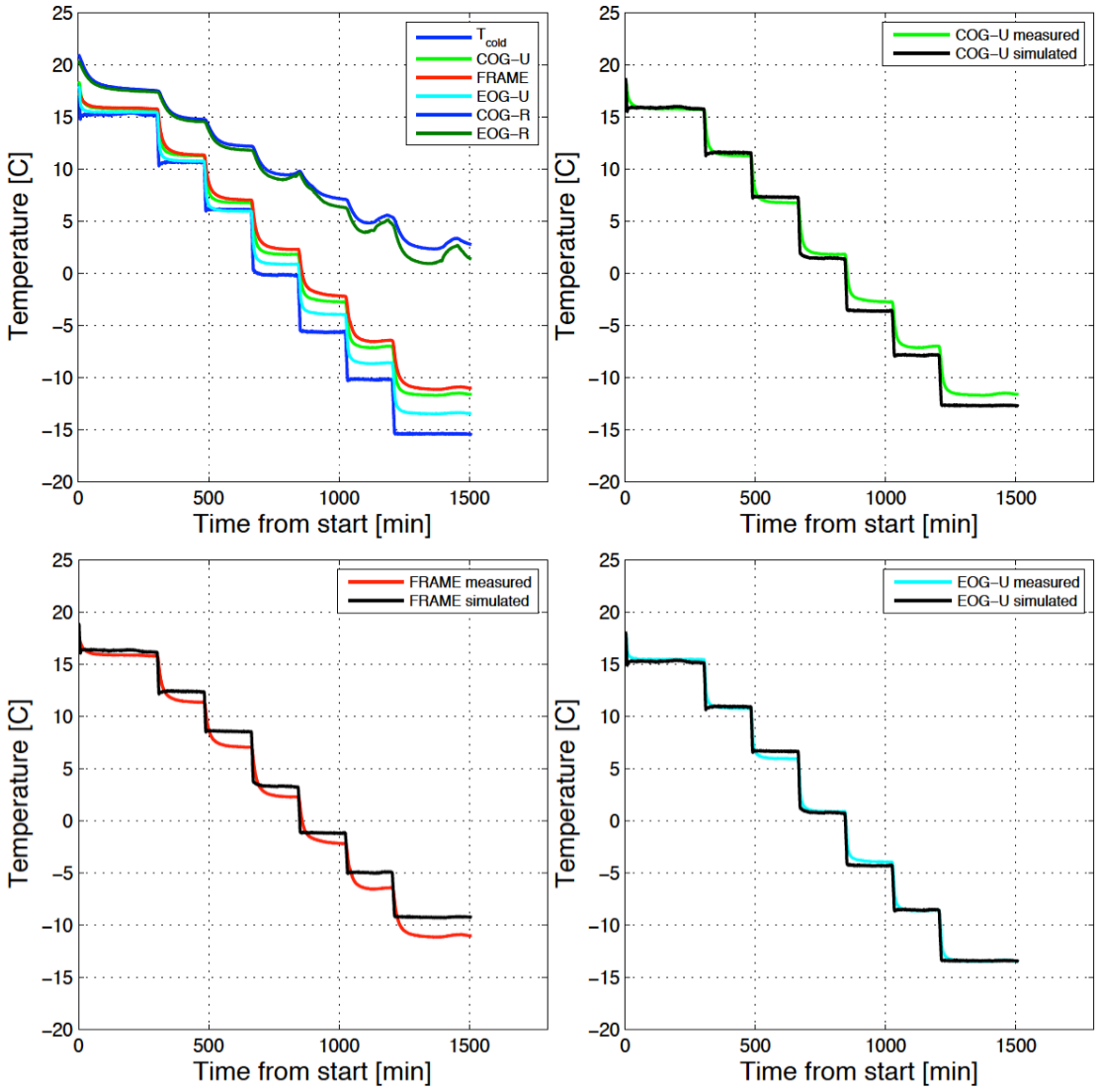

Figure 12. Measured surface temperatures on product G

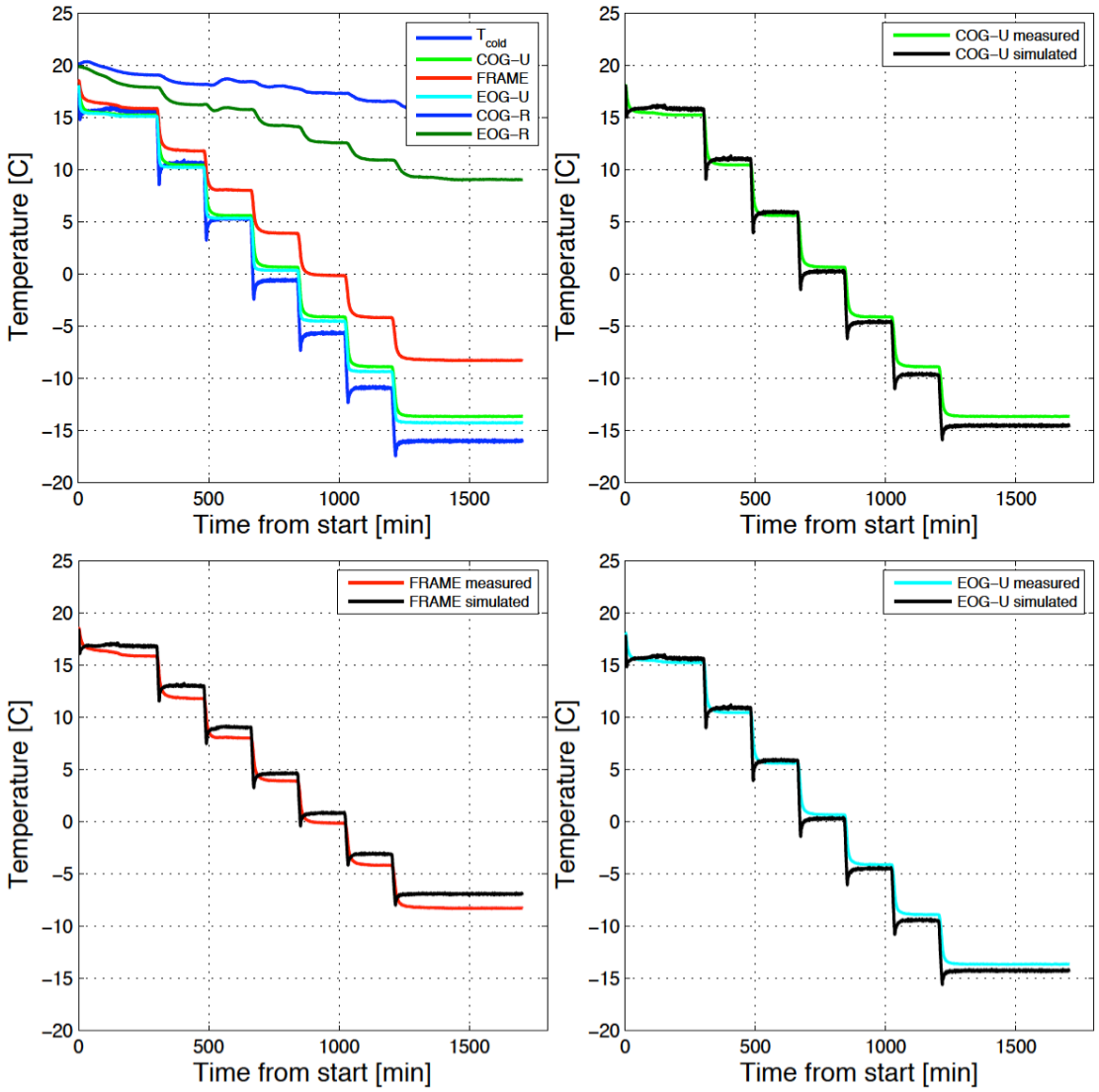

Figure 13. Measured surface temperatures on product A

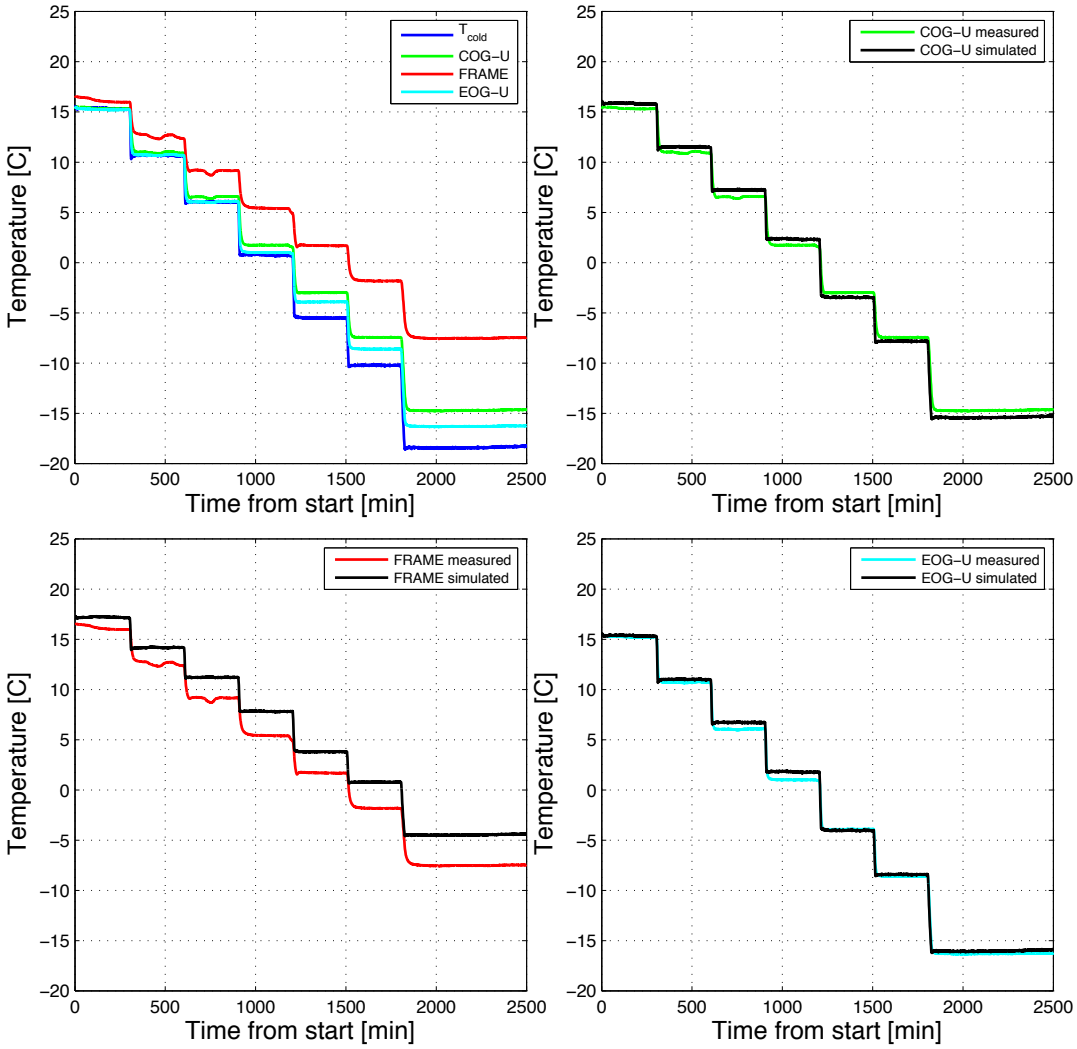

Figure 14. Measured surface temperatures on product I

Moisture transfer

Detailed measurements for product G are presented in Figure 15 to illustrate the process used to determine the water vapor diffusion resistance factor, μ. Figure 15a shows the adjacent room air humidity is brought quickly to 100% and then held at that point while moisture is allowed to diffuse into the between-glass space. Figure 15b shows the calculated partial water vapor pressures of each space. Figure 15c shows the calculated moisture content of the between glass space and a polynomial fit to the measurements. The polynomial fit is then used to determine μ, as is shown in Figure 15d. The average μ is determined from all data prior to any inflection point of moisture content, or when the between-glass space becomes saturated. This inflection point can be seen at approximately 2600 minutes in Figure 15c.

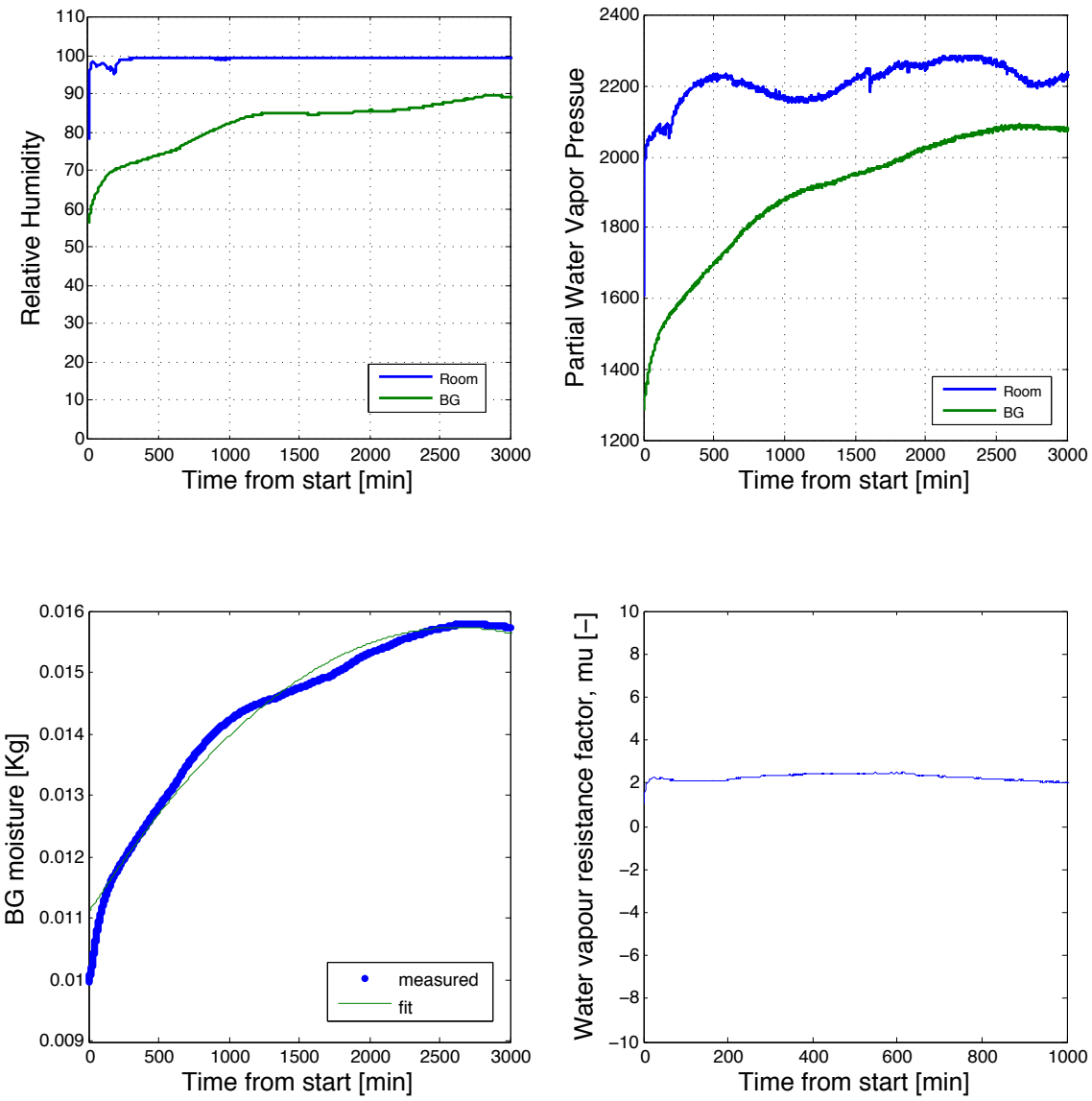

Figure 15a-d. Vapor diffusion measurement and calculation details for product G.

The process described above is repeated for all products listed in Table 2. Vent direction to the outside describes vapor diffusion through the base frame. The calculated diffusion coefficient for two tests is less than 1, meaning calculated moisture diffusion is faster than diffusion through air. This result is not possible without some unaccounted for pressure difference or air movement. A value of one is therefore used to represent as-measured performance of these tests in the subsequent building simulations. Based on the previous airflow measurements, the products perform as expected. Product A did not reduce airflow and also showed no resistance to moisture flow. Product G provided the greatest resistance to airflow and the greatest resistance to moisture flow.

Table 2. Vapor diffusion measurement summary

	Vent Direction	
Product	Outside	Inside
Base	0.3	-
A	10.6	0.6
G	-	2.3
I	-	1.8

Simulation

Condensation resistance

The simulated CR and CRU values for each window are shown in Table 5. Where the CRU calculation is not applicable because the system does not contain an unsealed gap, the field is left blank. It is clear from the CRU – Vented to the interior boundary condition (BC) that the condensation resistance is significantly decreased when an SGS product vents solely to room air. The primary driver for low CRU values is the temperature reduction on the base window glass coupled with the high dew point of room air. The significant surface temperature reductions can be seen in the test results when comparing Figures 10 (base window) to Figures 12 - 14. Many real building base windows are not completely sealed to outside air infiltration so the CRU for the unsealed gap vented to a mixture of exterior and interior air is also of interest.

Table 5. Simulated CR and CRU

Product	**CR**	**CRU Vented to interior BC**
Base	12.2	-
A	21.6	1.96
B	27.0	-
C	26.8	-
D	26.8	-
E	22.1	1.38
F	22.0	4.23
G	26.0	4.24
I	23.9	3.64
J	24.5	3.57

Figure 16 shows the simulated CRU for product F over a range of unsealed gap air humidity ratios. The humidity ratio of the simulated exterior boundary condition is around 0.001 Kg (H_2O)/Kg (dry air) as shown by the solid black vertical line, so a CRU of 100 is expected for all humidity ratios below that level since no condensation can occur. Since the SGS product shown insulates the base window glass and reduces its temperature, there is a highly non-linear drop in CRU once the humidity

ratio is increased above the exterior humidity ratio. This drop explains the relatively low CRU numbers reported in Table 5.

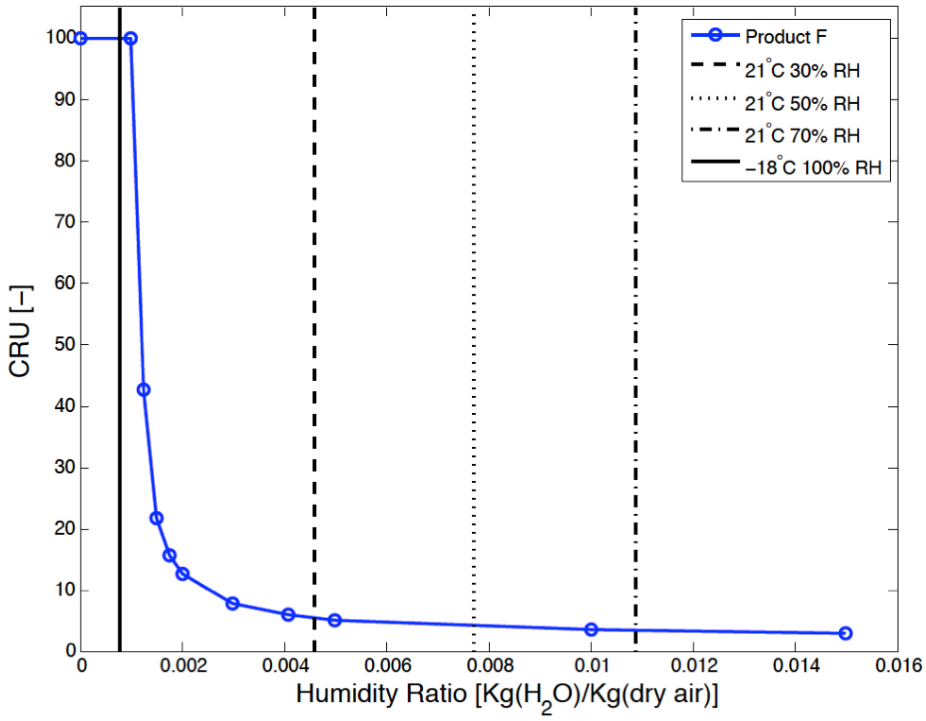

Figure 16. CRU for Product F as a function of unsealed gap humidity ratio

Whole building

The annual whole building condensation simulation results can be parsed in many ways. Three different methods are presented here. The large office in Missoula Mt with product A is used to represent a typical result of the analysis in the following figures. Figure 7 shows the accumulated 15-minute time steps when condensation occurs to provide an idea of total condensation risk over time. For the case shown, and typically for all units examined, we observe that condensation risk is greatest within the first and last 100 days of the calendar year. East facing windows have the lowest condensation risk, while north facing has the greatest risk. North facing windows are rarely exposed to direct sun and the associated surface heating, so this result aligns with our intuition. South, east, and west windows perform similarly in winter and fall (first 50 days and last 100 days of year). East windows though show fewer summer condensation hours.

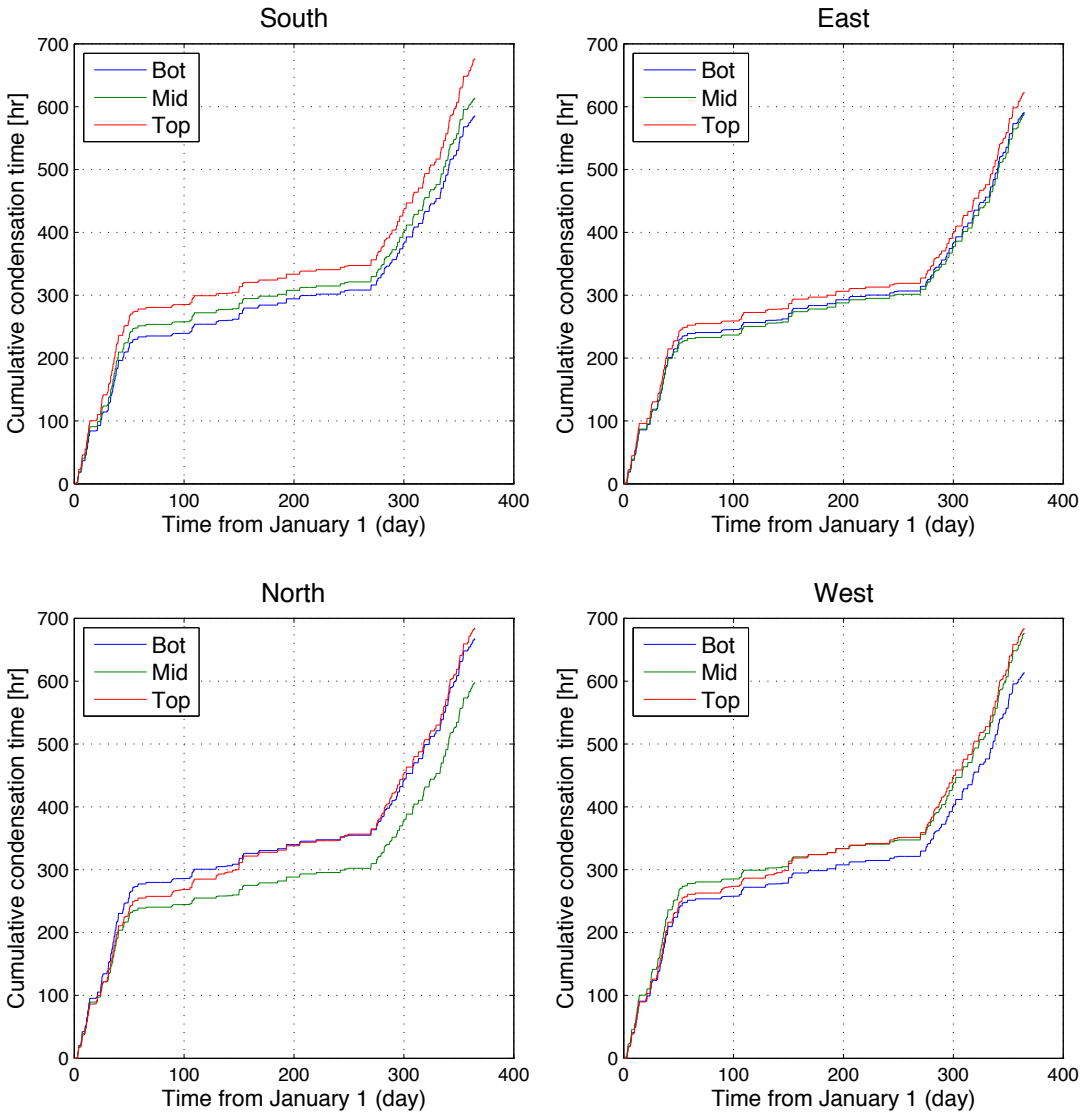

Figure 17. Accumulated condensation time. Large office, Missoula M, product A.

The reduced condensation hours on east windows in summer can be attributed to solar heating of those windows from morning sun. Figure 18 shows this by splitting the cumulative condensation hours by hour of day and direction. For the majority of hours all four surfaces are similar. From 7am – 10am though, both the south and east facing windows have significantly fewer condensed hours than north and west facing. The east facing windows also show fewer condensed hours relative to south facing, primarily in the 7am and 8am hours.

An additional significant observation made from Figure 18 is the day to night condensation deviation for all orientations. From late morning to late afternoon little to no condensation occurs. Starting in late afternoon, the likelihood of condensation increases each hour until it reaches a peak in hours 4 and 5. At hour 6 condensation risk quickly diminishes until hour 11 where the risk returns to minimal. The strongest correlation to the condensation pattern seen is the outdoor

air temperature. This correlation is shown in Figure 18 with a line graph of the inverse to mean temperature at each hour. Each building is run on a 7am – 10pm HVAC schedule and there is no visible correlation seen in the HVAC schedule to condensation risk.

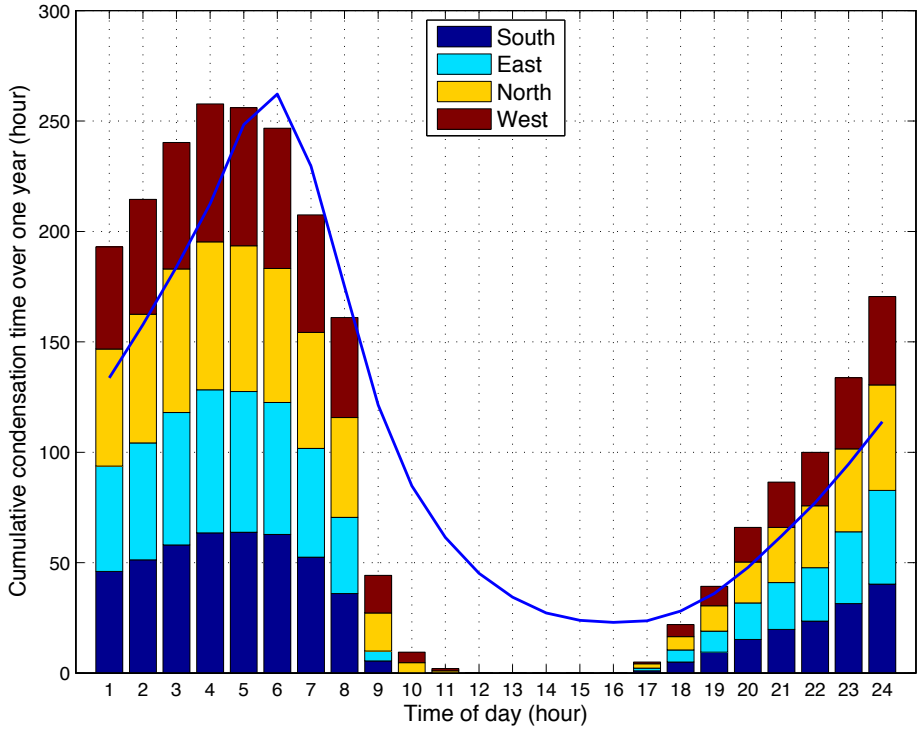

Figure 18. Cumulative condensation hours by hour of day and direction. Large office, mid floor, Missoula M, product A.

The detailed analysis shown above is useful for understanding condensation trends in all products. To understand how products compare relative to each other summarized results are used. One of the largest issues with condensation is view during occupied periods. Summarized condensation hours based on a typical building schedule with open hours of 7am – 7pm and the measured moisture diffusion properties are provided in Figures 19-21. The measured water vapor diffusion resistance factors are used in the analysis. Where measured factors are not available a representative value of μ_{in}=2 is used for room side diffusion and μ_{out}=10.6 for outside diffusion. The figures show that little to no condensation occurs on the base window or products B, C, and D. Each of these products has a sealed cavity, or a room-side condensation surface. For all other products, condensation hours are dominantly during non-business hours. The SGS product U-factor correlates most closely with condensation hours, where lower u-factors have higher condensation potential. This observation applies only to the SGS products with unsealed cavities.

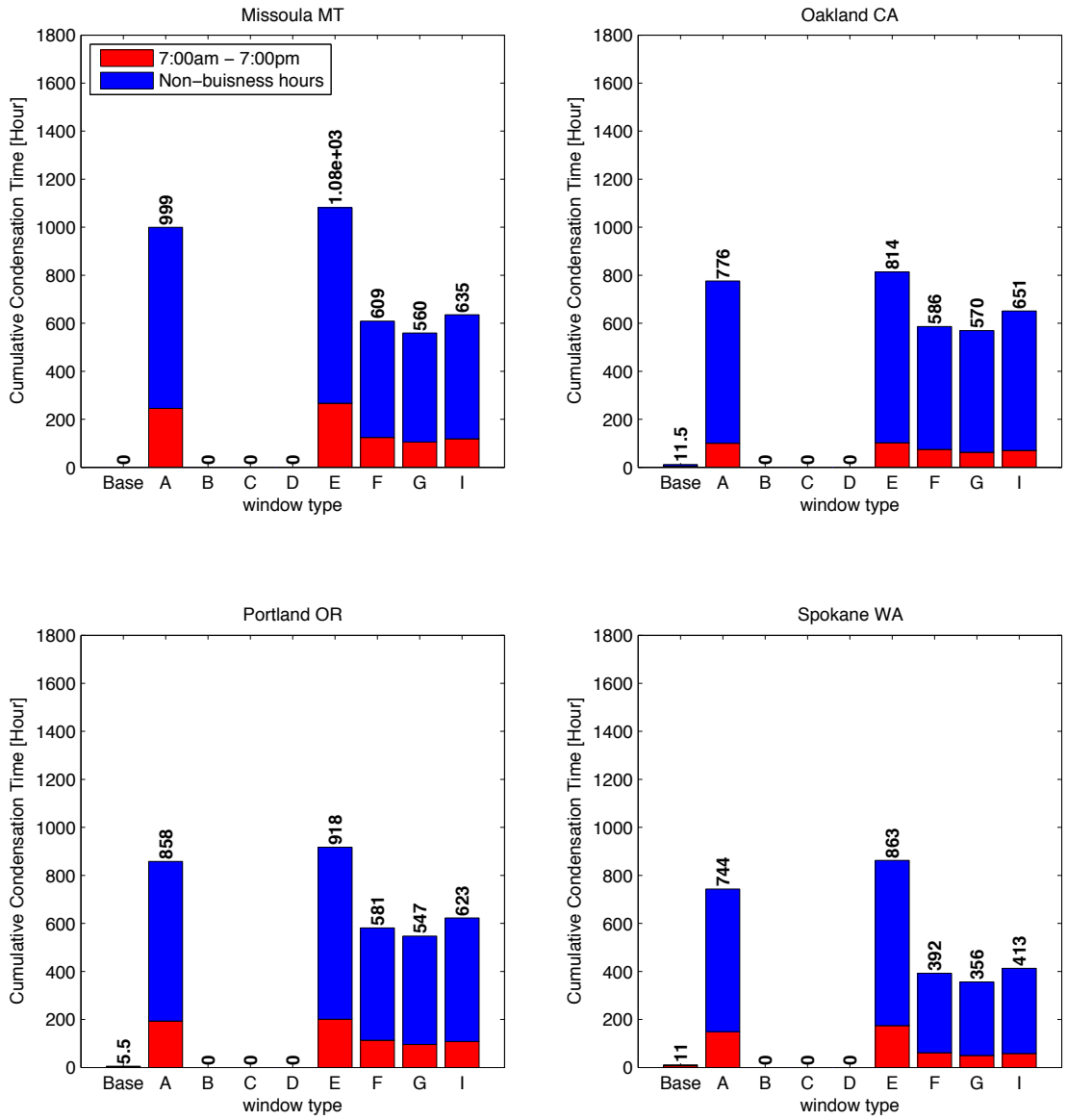

Figure 19. Small office total condensation hours based on typical building schedule.

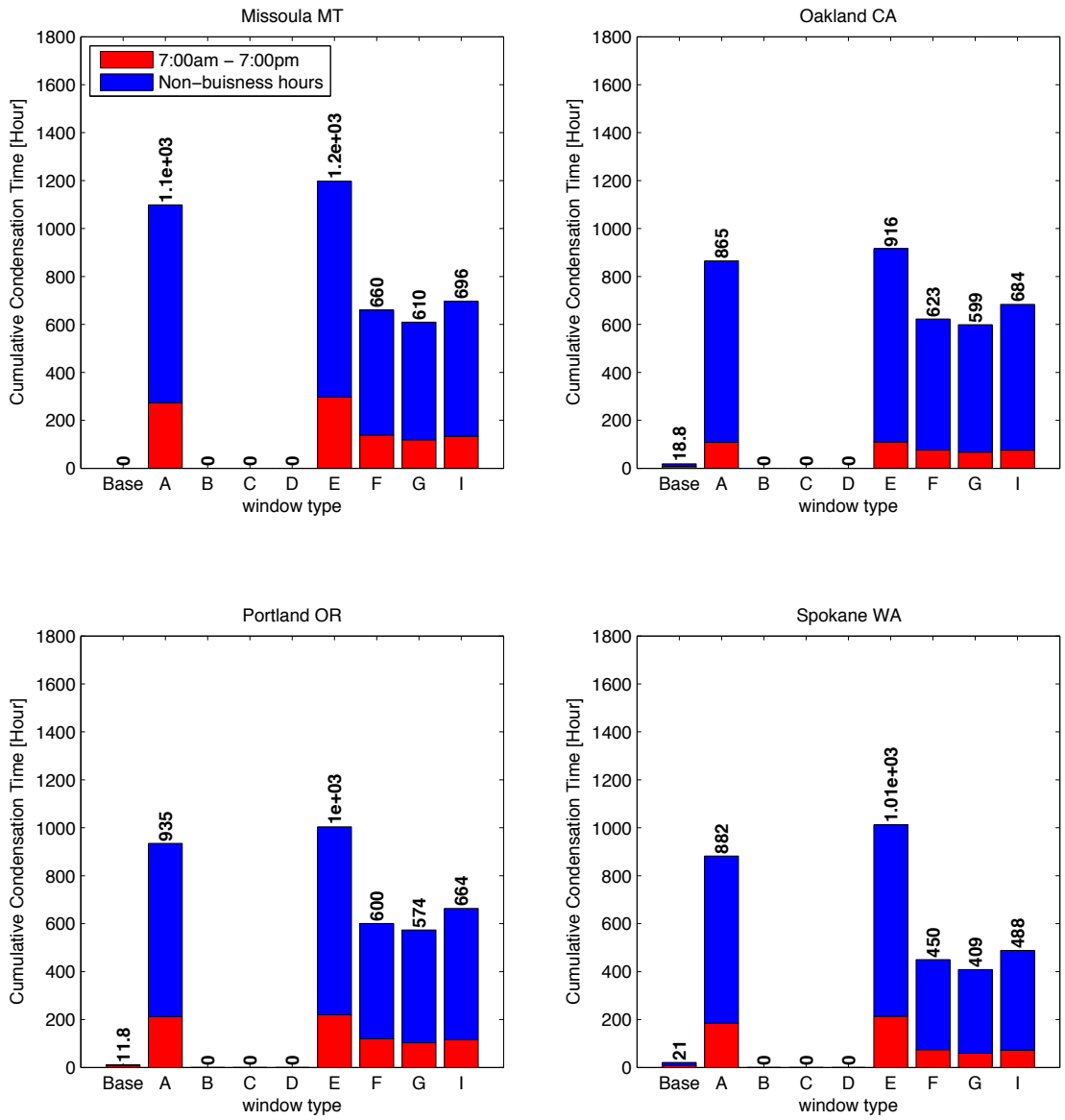

Figure 20. Medium office total condensation hours based on typical building schedule.

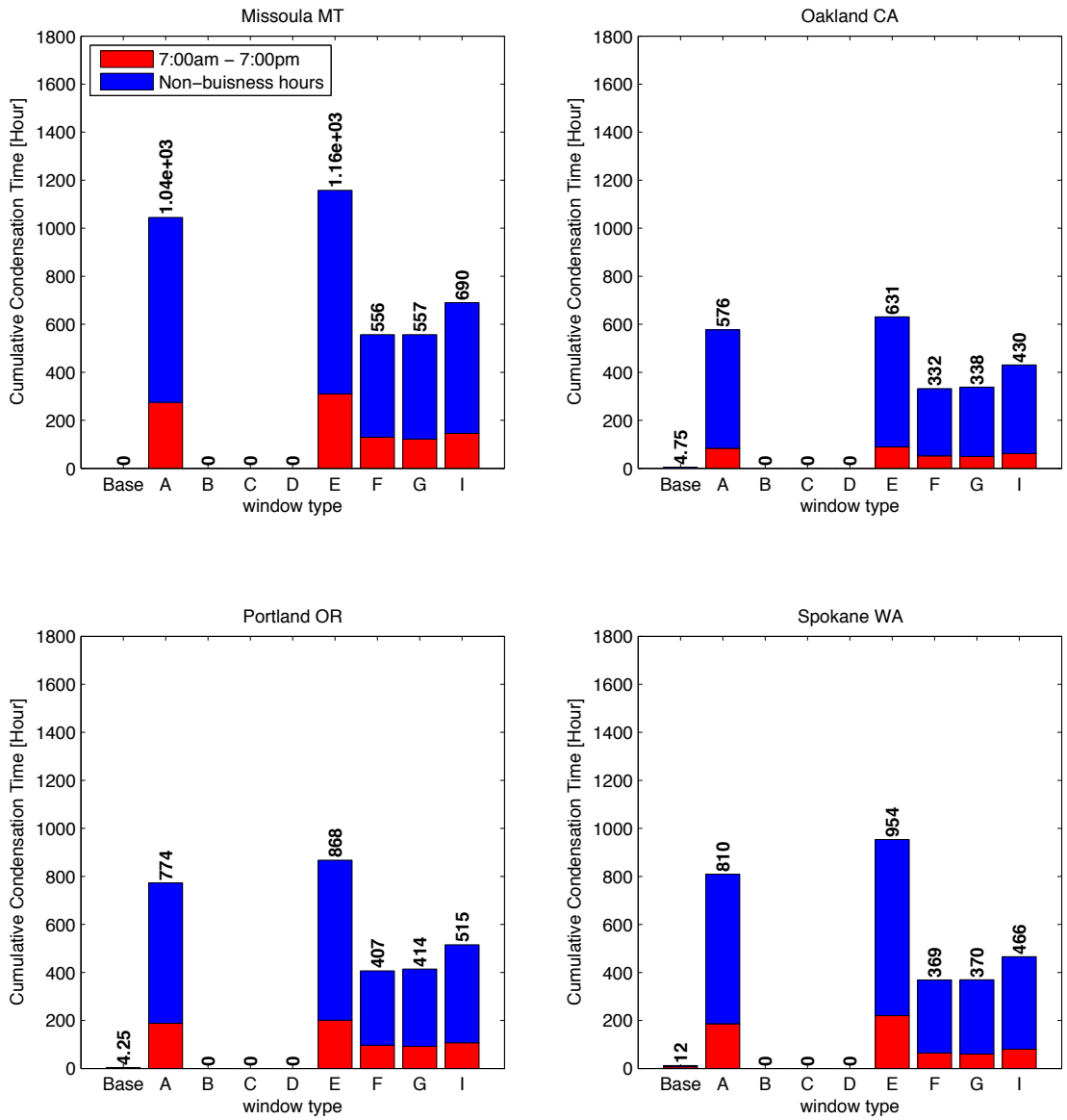

Figure 21. Large office total condensation hours based on typical building schedule.

The previous results were for measured water vapor diffusion resistance factors. In order to illustrate the impact of μ on condensation hours, Figure 22 shows a comparison of non-business hour total condensation based on five different μ_{in} and μ_{out} combinations in large office buildings. The plots show that low resistance to the outside coupled with high room-side resistance typically results in the fewest condensation hours, while the opposite case (high resistance to the outside and low resistance room-side) results in the greatest number of condensation hours. In the case where resistance is quite high in both directions, the initial moisture content of the space is very important. In the extreme, no initial moisture content is present (similar to a sealed cavity) and condensation never occurs. Low initial moisture is

used in this analysis at 1/10 of the room moisture on the first 15-minute time step of January 1.

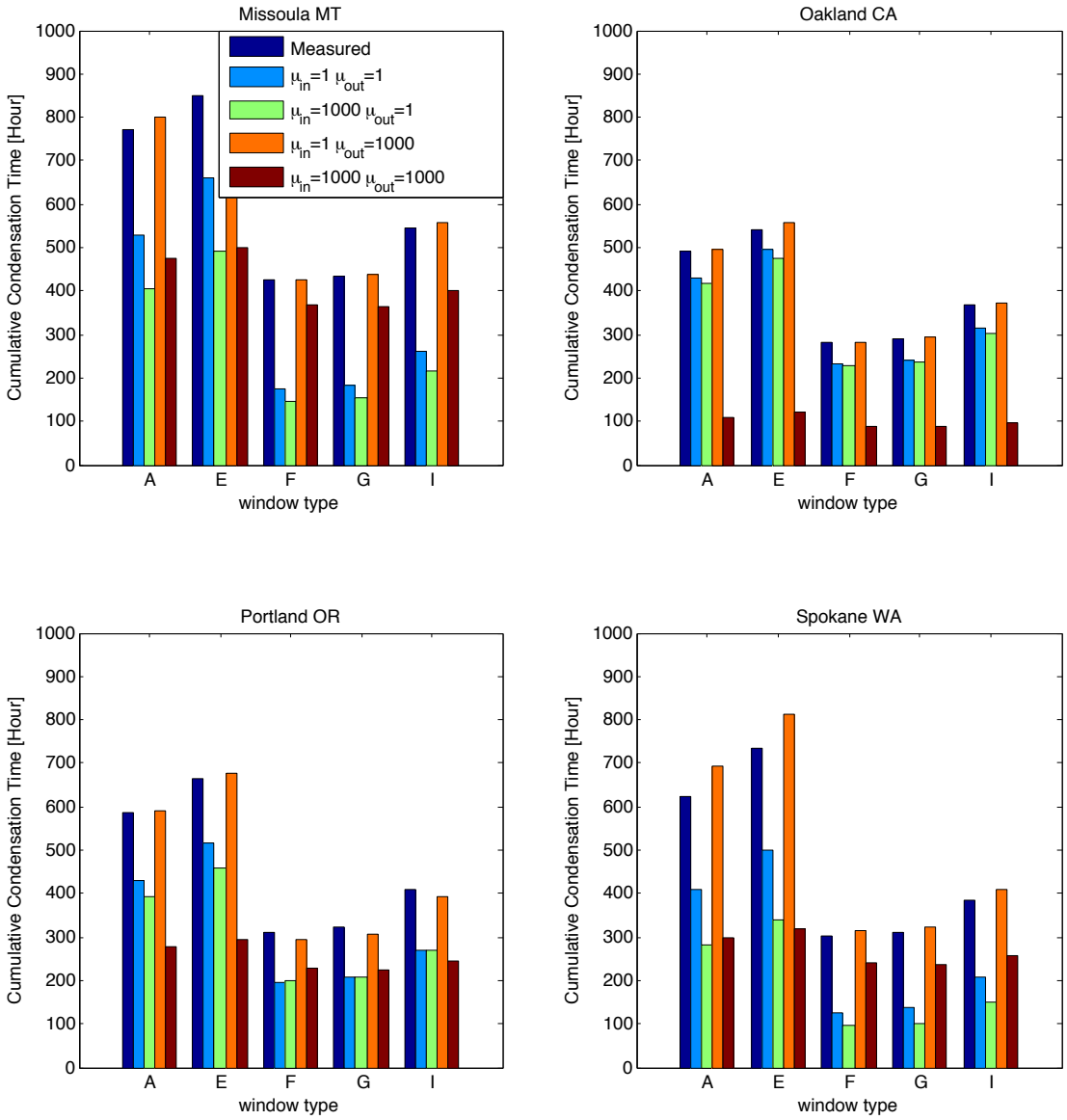

Figure 22. Condensation time for different inside and outside water vapor diffusion resistance factor combinations. Large Office, non-business hours.

5. SUMMARY & CONCLUSIONS

A refined methodology for simulating the hygrothermal conditions adjacent to and on glass surfaces is developed and performed for nine products as an extension to the work presented in Hart, 2005. Extensions to Berkeley Lab THERM and WINDOW software tools are implemented and we introduce the concept of condensation resistance of unsealed gaps (CRU) indices as a companion to the existing NFRC CR ratings. These models are validated through experiments by local temperature and moisture propagation measurements, and therefore provide accurate determination

of CRU at predetermined humidity ratios. The reported CRU numbers seem to be mostly on the very low end (i.e., very poor performance) for all unsealed units due to the use of humidity ratios that are representative of indoor room air. This indicates that further research might be needed to establish expected moisture content in unsealed gaps for different product types and to relate them to indoor room air, so that more representative CRU procedure can be developed.

Four SGS systems are measured for air leakage and moisture propagation performance. The results vary greatly between products; from preventing all air leakage and most moisture transfer to no resistance to air or moisture transfer. The measured performance data is combined with the results of Energy Plus annual energy simulations to determine trends and relative condensation performance of nine SGS products. We make the assumption that there are no moisture sources or sinks, and there is no liquid transport flux. Both of these assumptions are significant in that condensed moisture is considered out of the system, potentially misjudging the condensation time. With these assumptions and knowing that all buildings are controlled and perform differently, the results presented here should be viewed only as indicators of relative performance between SGS products and not absolute condensation potential.

The results show that all SGS systems containing unsealed glazing cavities increase condensation risk over single pane base windows. Condensation risk is highest on north facing surfaces, and lowest on east facing, but the time difference is relatively small. Condensation also occurs most often during unoccupied hours. Finally, low water vapor diffusion resistance factors to the outside coupled with high room-side resistance typically results in the fewest condensation hours, while the opposite case (high resistance to the outside and low resistance room-side) results in the greatest number of condensation hours.

Future work should include installation and monitoring of SGS in real buildings to validate the simulation results. The CRU metric is introduced as a preliminary step with the long-term goal of a standardized metric for condensation potential of SGS and other attachment products. Further development of the CRU metric should be done to ensure all significant aspects of SGS design, such as resistance to air leakage and moisture transfer, are considered and presented fairly with respect to the existing CR standards.

6. ACKNOWLEDGEMENT

This work was supported by the Northwest Energy Efficiency Alliance (NEEA) and the Assistant Secretary for Energy Efficiency and Renewable Energy, Building Technologies Program, of the U.S. Department of Energy under Contract No. DE-AC02-05CH11231.

7. REFERENCES

American Architectural Manufacturers Association (AAMA), 2008. *AAMA/WDMA/CSA 101/I.S.2/A440 NAFS – North American Fenestration Standard/Specification for Windows, Doors, and Skylights.* Schaumburg, Il.

AAMA, 1998. *Guidelines For AAMA Accreditation Of Independent Laboratories Performing On-Site Testing Of Fenestration Products.* Schaumburg, Il.

American Society of Heating, Refrigerating, and Air-Conditioning Engineers, Inc. (ASHRAE), 2009. *Handbook of Fundamentals*, Atlanta, GA.

ASTM Standard E283, 2012. *Standard Test Method for Determining the Rate of Air Leakage Through Exterior Windows, Curtain Walls, and Doors Under Specified Pressure Differences Across the Specimen*, ASTM International, West Conshohocken, PA.

Fraunhofer-Gesellschaft, 2001. *WUFI BIO*. The Fraunhofer Institute for Building Physics. München, Germany.

Hart, Robert, H. Goudey, R. Mitchell, M. Yazdanian, D.C. Curcija. 2015. *Secondary Glazing System (SGS) Thermal, Moisture, and Solar Performance Analysis and validation.* Northwest Energy Efficiency Alliance. Report #E15-293.

ISO 12572, 2001. *Hygrothermal performance of building materials and products--Determination of water vapour transmission properties.*

Kunzel, Hartwig M., 1995. *Simultaneous Heat and Moisture Transport in Building Components*. The Fraunhofer Institute of Building Physics. München, Germany.

Mitchell, R., Kohler, C., Curcija, D., Zhu, L., Vidanovic, S., Czarnecki, S., et al. (2013). *THERM 6.3 / WINDOW 6.3 NFRC Simulation Manual.* Lawrence Berkeley National Laboratory. Berkeley, CA: University of California.

U.S. Department of Energy. (2013, October 30). *EnergyPlus Energy Simulation Software*. Retrieved January 12, 2015, from US DOE Energy Efficiency & Renewable Energy web site: http://apps1.eere.energy.gov/buildings/energyplus/energyplus_about.cfm

The National Renewable Energy Laboratory. (2015, January 19). *National Solar Radiation Data Base*. Retrieved January 21, 2015, from Renewable Resource Data Center: http://rredc.nrel.gov/solar/old_data/nsrdb/1991-2005/tmy3/

8. APPENDIX 1

The numerical process to determine if condensation occurs between-glass is described in this section. This process is used to develop the results presented in the simulation section of the results. Unless otherwise noted, all referenced equations are taken from ASHRAE 2009 and presented in the form F#.# for (F)undamentals, chapter.equation.

1. Window models are defined using BSDF idf inputs for Energy Plus. This is required to obtain glass surface temperatures. These files were produced in Berkeley Lab WINDOW 7.3 for this work.
2. 15-minute time step Energy Plus simulation is performed. The following outputs are required for all simulations. Zone data is required for each perimeter zone.

t	Date/Time
T_{out}	Environment:Site Outdoor Air Drybulb Temperature [C]
T_{out_dp}	Environment:Site Outdoor Air Dewpoint Temperature [C]
P_{out}	Environment:Site Outdoor Air Barometric Pressure [Pa]
T_{in}	Zone Air Temperature [C]
ϕ_{in}	Zone Air Relative Humidity [%]
w_{in}	Zone Mean Air Humidity Ratio [kgWater/kgDryAir]
T_{S2}	Surface Window Back Face Temperature Layer 1 [C]
T_{S3}	Surface Window Front Face Temperature Layer 2 [C]

3. For each 15 minute timestep:
   3.1. Calculate P_{ws_in} by using the following equations F1.5-6, given the input of T_{in} [K] from Energy Plus:

For −100< T > 0°C

$$\ln P_{ws} = C_1/T + C_2 + C_3T + C_4T^2 + C_5T^3 + C_6T^4 + C_7 \ln T$$

For 0< T > 200°C

$$\ln P_{ws} = C_8/T + C_9 + C_{10}T + C_{11}T^2 + C_{12}T^3 + C_{13} \ln T$$

where

C_1 = −5.6745359 E+03
C_2 = 6.3925247 E+00
C_3 = −9.6778430 E−03
C_4 = 6.2215701 E−07
C_5 = 2.0747825 E−09
C_6 = −9.4840240 E−13
C_7 = 4.1635019 E+00
C_8 = −5.8002206 E+03
C_9 = 1.3914993 E+00
C_{10} = −4.8640239 E−02
C_{11} = 4.1764768 E−05
C_{12} = −1.4452093 E−08

C_{13} = 6.5459673 E+00
P_{ws} [Pa] saturation pressure

3.2. Calculate P_{w_in} by using equation F1.24, given the input of ϕ_{in} [-] from Energy Plus:

$$\phi = \frac{P_w}{P_{ws}}\Big|_{T,P}$$

3.3. Calculate T_{in_dp} by using equation F1.39-40, given the input of P_{w_in} from 3.2:

For $T_{dp} \leq 0°C$

$$T_{dp} = 6.09 + 12.608\alpha + 0.4959\alpha^2$$

For $0 < T_{dp} > 93°C$

$$T_{dp} = C_{14} + C_{15}\alpha + C_{16}\alpha^2 + C_{17}\alpha^3 + C_{18}P_w^{0.1984}$$

where
$\alpha = \ln(P_w)$;
C14 = 6.54
C15 = 14.526
C16 = 0.7389
C17 = 0.09486
C18 = 0.4569

3.4. Calculate P_{in} by using equation F1.22, given the input of P_{w_in} from 3.2 and w_{in} from Energy Plus:

$$P = P_W\left(1 + \frac{w}{0.621945}\right)$$

3.5. Calculate P_{BG} by taking the average of P_{in} from 3.4 and P_{out} from Energy Plus:

$$P_{BG} = \frac{P_{in} + P_{out}}{2}$$

3.6. Calculate P_{w_out} by using the input of T_{out_dp} from Energy Plus and equation from 3.1, where $P_w = P_{ws}(T_{dp})$.

3.7. Calculate W_{out} by using the inputs of P_{out} from E+ and P_{w_out} from 3.6, and equation from 3.4 rearranged to solve for W.

$$W = 0.621945\left(\frac{P_w}{P - P_w}\right)$$

3.8. Calculate T_{BG} by taking the average temperature between T_{S2} and T_{S3} from Energy Plus.

$$T_{BG} = \frac{T_{S2} + T_{S3}}{2}$$

3.9. Calculation of T_{BG_dew} is an iterative process by looping through 3.9.1 – 3.9.3 for each time step.

3.9.1. $W\rho_{BG}$ at each time step is solved for by utilizing the following equations:

$$(W \cdot \rho_a)_{t2} = (W \cdot \rho_a)_{t1} + \delta(t_2 - t_1)\left[\left(\frac{P_{w\_in} - P_{w\_BG}}{\mu_{in} \cdot \Delta x^2}\right)_{t1} + \left(\frac{P_{w\_out} - P_{w\_BG}}{\mu_{out} \cdot \Delta x^2}\right)_{t1}\right]$$

$$\delta = 2.0 \cdot 10^{-7} \, (T_{BG}^{0.81})_{t2} / (P_{BG})_{t2}$$

at t = 1

$$W_{BG} = \frac{W_{in} + W_{out}}{2}$$

$$(W \cdot \rho_a) = W_{BG} \cdot \rho_a$$

$$P_W = \frac{P \cdot W_{BG}}{(0.621945 + W_{BG})}$$

3.9.2. Calculate W_{BG} at each time step by dividing $W\rho_{BG}$ by the air density.

$$W = \frac{(W \cdot \rho_a)}{\rho_a}$$

3.9.3. Calculate P_{w_BG} at each time step by equation from 3.4 rearranged to solve for partial water pressure.

$$P_{W\_BG} = \frac{P \cdot W_{BG}}{(0.621945 + W_{BG})}$$

3.10. After P_{w_BG} is determined for each time step, T_{BG_dew} is solved for using equation from 3.3.

3.11. Surface condensation is then determined by comparing T_{BG_dew} to the glass surface temperature at each time step. If surface temperature is below the space dew point temperature the surface contains condensation at that time step.